A Model of Learning Axonal Conduction Delays, Representative of Adaptive Myelination

A THESIS

submitted by

Meenakshi Asokan

for the award of the degree of

Bachelor of Technology

DEPARTMENT OF ELECTRICAL ENGINEERING
INDIAN INSTITUTE OF TECHNOLOGY MADRAS,
CHENNAI 600 036

MAY 2015

THESIS CERTIFICATE

This is to certify that the thesis titled **A Model of Learning Axonal Conduction Delays, Representative of Adaptive Myelination**, submitted by **Meenakshi Asokan**, to the Indian Institute of Technology, Madras, for the award of the degree of **Bachelor of Technology**, is a bona fide record of the research work done by her under our supervision. The contents of this thesis, in full or in parts, have not been submitted to any other Institute or University for the award of any degree or diploma.

V. Srinivasa Chakravarthy
Research Guide
Professor
Computational Neuroscience Laboratory
Bhupat and Jyoti Mehta School of Biosciences Building
IIT Madras, Chennai – 600036

Krishna Vasudevan
Research Co-Guide
Professor
Department of Electrical Engineering
IIT Madras, Chennai – 600036

Place: Chennai

Date:

ACKNOWLEDGEMENTS

I would like to thank Prof. V.Srinivasa Chakravarthy for giving me the invaluable opportunity to do this research work under his guidance. The interest that he took in my progress has been a great motivating factor for me. I would also like to thank my co-guide Prof. Krishna Vasudevan for his support. I would like to express my gratitude to Karishma Chhabria, MS Scholar for her suggestions and for listening to me patiently every time I hit the wrong end. I am also deeply indebted to all other members of the group for always being there to offer words of advice and for all the enlightening discussions. To my parents, I am extremely grateful for helping me survive the stress and for their unconditional love.

Abstract

Learning and plasticity in the brain has generally been attributed to synaptic weights in the neuronal network. But recent studies and experiments provide evidence for the fact that axonal conduction delays are also dynamic variables that add a novel dimension to the information processing in the brain. This is attributed to the adaptive myelination brought about by oligodendrocytes, glial cells that myelinate the axons in the central nervous system.

As a part of this project, we have proposed that these axonal conduction delays could be trained in addition to training the synaptic weights, in response to dynamic input spike patters. After reviewing the various mechanisms that could be underpinning the activity dependent myelin plasticity, the role of electrical impulses and their timings was made clear. Consequently we came up with an algorithm that is dependent on the spike timings to train these delays. Further, we used motion perception as a tool to test the usefulness of the algorithm in assessing and studying myelin plasticity. Our model emphasizes that myelination is no simple electrical insulation, but rather an exquisite way of controlling complex dynamic functions and by adding this supplementary dimension to the neuronal network, we inch one step closer to a neuro-biologically realistic model of the brain.

Adaptive changes in myelin forming cells and myelin sheath thickness and thereby the conduction velocity represents a type of behaviorally relevant neural plasticity that could indeed be leveraged for interventions in diseases of myelin. Human diseases such as Multiple Sclerosis (MS) and inherited leukodystrophies in which the integrity of myelin sheath is lost, make the importance of myelin for Central Nervous System (CNS) functioning all the more apparent. Given that recent studies are demonstrating an unprecedented level of myelin plasticity in the adult CNS, identifying the mechanism that promotes or inhibits myelination during development could aid in the goal of developing novel strategies to promote repair in the demyelinated CNS. Especially if impulse activity could influence myelination even at later stages of oligodendrocyte development, this could have immense relevance to treating demyelinating diseases. Computational models of neuronal networks that learn temporal delays is a major step towards modeling adaptive myelination and consequently a way to explore the various parameters that influence myelin plasticity that could be of relevance to treating diseases of myelin.

Contents

List of Figures

Abbreviations

AP	-	Action Potential
CNS	-	Central Nervous System
CV	-	Conduction Velocity
DTI	-	Diffusion Tensor Imaging
EPSP	-	Excitatory Post Synaptic Potential
FA	-	Fractional Anisotropy
IPSP	-	Inhibitory Post Synaptic Potential
LIF	-	Leaky Integrate and Fire
LTD	-	Long Term Depression
LTP	-	Long Term Potentiation
MBP	-	Myelin Basic Protein
MIMO	-	Mutliple Input Multiple Output
MRI	-	Magnetic Resonance Imaging
ON	-	Optic Neuritis
OPC	-	Oligodendrocyte Precursor Cells
PFC	-	PreFrontal Cortex
PSP	-	Post Synaptic Potential
RT	-	Reaction Time
SOM	-	Self Organizing Map
STDP	-	Spike Timing Dependent Plasticity
STDMP	-	Spike Timing Dependent Myelin Plasticity
VEP	-	Visually Evoked Potential

Chapter 1

Background Information

1.1 Computational Neuroscience

Computational neuroscience is the study of brain function in terms of the information processing properties of the fundamental components of our brain. It is an interdisciplinary science that links the diverse fields of neuroscience, cognitive science, and psychology with electrical engineering, computer science, mathematics, and physics.

It encompasses two approaches to model the brain functions. On one hand, it makes it possible to create biophysically realistic models by writing a computer program to simulate the operation of a network of cells in the brain by making use of system of equations that describe their electrical and chemical signaling. On the other hand, it is possible to study how the brain performs computation by simulating, or mathematically analyzing, the operations of simplified "units" that have some of the properties of neurons but abstract out much of their biological complexity. Since the biophysically realistic models can get extremely complex and computationally challenging, computational neuroscientists constantly try to strike a balance between neurobiological realism with reliable and convenient abstraction.

1.2 Human Brain

Like every other organ, the brain is made up of cells and the cells in the brain fall into two broad classes: neurons and glial cells. But the brain's network of cells forms a massively parallel information processing system that makes understanding the brain very different from understanding other organs in the body. Events in a silicon chip happen in nanosecond range, whereas neural events happen in the millisecond range. However, the brain makes up for the relatively slow rate of operation by having a truly staggering number of neurons with massive interconnections between them. An adult brain consists of about 100 billion neurons with each having about 1000-10,000 connections and in total 3.2 million km of wires, all packed into 1.5 liters and weighing 1.5 kg. Yet, the brain is an enormously

efficient structure, consuming only the same amount of electric power as a night-light!

1.3 Neuron

1.3.1 Morphology & Structure

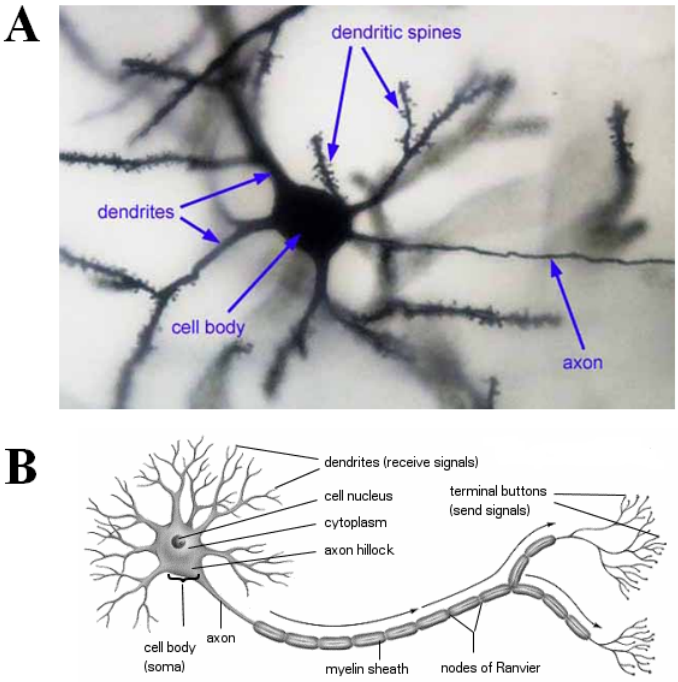

Figure 1.1: **A:** A golgi stained neuron in layer II of cerebral cortex [*Adapted from http://www.siumed.edu/ dking2/ssb/BH004b.htm*] **B:** A diagram depicting the structure of a neuron

Neurons are a class of cells that distinguish themselves from most other cells through the elaborate wiring that emerges from their cell body, also called soma which contains the nucleus and other organelles necessary for cellular function. From Figure 1.1 it can be seen that the short and densely distributed wiring known as dendrites receive signals from other neurons and typically, a single long wire known as axon branches into smaller axon terminals and transmits the signal. An axon arises from the cell body at the axon hillock and travels for a distance, as far as 1 meter in humans. One neuron connects to another neuron through the synapse, a small gap between the axon terminal of one neuron and the dendrite of another. The electrical signal that travels through the axon is transmitted as a chemical message across the synapse. It has been estimated that one neuron can receive contacts from up to 10,000 other cells. Similarly, any one neuron can contact up to 10,000 post-synaptic cells. Thus, this fundamental component of the nervous system can be thought of as a Multiple Input Multiple Output (MIMO) information processing unit.

1.3.2 Electrophysiology

A voltage difference is maintained between the interior of a neuron and its extracellular space due to the difference in the concentration of ions such as Na^+, K^+, Cl^-, Ca^{2+}. In resting conditions this voltage gradient/ membrane potential is about -70 mV. But all neurons are electrically active: On appropriate stimulation, the membrane potential varies, carrying signals that can be transmitted from one neuron to another. This is facilitated through ion channels, membrane proteins that allow transport of specific ions. Special types of voltage gated ion channels trigger a sharp voltage spike called an Action Potential (AP), also known as nerve impulse or spike. Neurons exhibit a characteristic known as excitability: APs are triggered only when the membrane is depolarized enough upto a threshold. Once elicited, it follows a consistent trajectory lasting about a thousandth of a second and hence it is known as the "all or none" response.

1.3.3 Stages of Neural Signaling

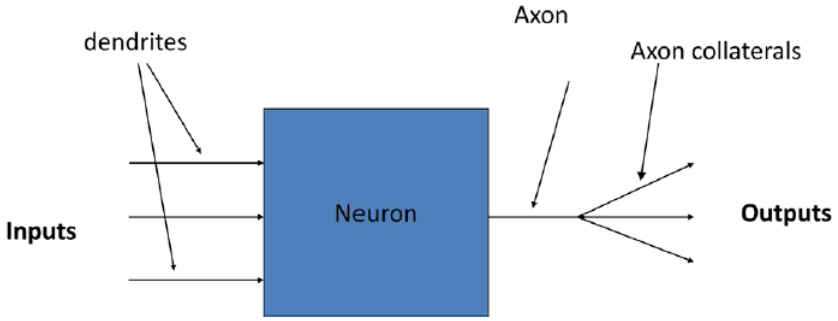

Figure 1.2: Neuron as a Multiple Input Multiple Output (MIMO) information processing unit

Figure 1.2 shows a neuron as a MIMO system. Inputs are received from other neurons by the dendritic tree and the output generated by the neuron is broadcast to other neurons by the axon collaterals. Neural signals are both electrical and chemical depending on the site of the signal transmission. The various stages of neural signaling are as follows (The first three are electrical and the last one is mostly chemical):

- **Propagation along the denritic tree**: A lossy propagation of a voltage change that could be both positive or negative depending on the nature of the synapse.
- **Summation at the axon hillock**: The voltage waves arising from the dendritic arbor gets integrated at the soma. The summation happens both spatially (summation of voltage waves from different dendrites) and temporally (summation of voltage waves even from the same dendrite which are overlapping in time). The axon hillock has high concentration of Na^+ and K^+ channels and hence gives rise to a "all or

none" response depending on whether the strength of the summation of the voltage waves crosses a threshold or not.

- **Action potential propagation along the axon and its collaterals**: The AP produced at the axon hillock propagates along the axon and reaches the collaterals. Most importantly, it propagates intact, without losing amplitude or spreading in time owing to the myelin sheath and saltatory conduction more about which can be found in Section 1.5.2.

- **Transmission of the signal across synapse**: Synapses can be electrical or chemical. Electrical synapses are direct cell-cell contacts mediated by gap junctions wherein the signaling is through exchange of ions. In a chemical synapse, when an AP arrives at an axon terminal, a chemical called neurotransmitter is released and it diffuses through the 20 nm gap called the synaptic cleft. The neurotransmitters could be excitatory or inhibitory depending on whether they produce a positive coltage change (Excitatory Post Synaptic Potential [EPSP])or a negative voltage change (Inhibitory Post Synaptic Potential [IPSP])in the dendrite. The exocytosis of the neurotransmitter is a probabilistic event and hence every AP needn't necessarily produce a PSP. Hence synaptic strength could be defined as average PSP produced in response to an AP on the presynaptic side.

1.4 Glial Cells

For decades, physiologists focused on neurons as the brain's prime communicators. Neuroglia or simply glia (latin for glue) were considered as the name suggests to hold the nervous system together in some way. Even though they outnumber nerve cells, they were thought to have only a maintenance role: bringing nutrients from blood vessels to neurons, maintaining a physiological balance of ions in the brain, and warding off pathogens that evaded the immune system. But it is recently being shown that glial cells may be as critical to thinking and learning as neurons are. Without their supportive functions, the signaling abilities of the neurons would be disrupted. Moreover comparison of brains reveals that the proportion of glia to neurons increases greatly in certain regions of the brain as animals move up the evolutionary ladder. It was indeed established that what distinguished Einstein's brain from a normal brain was the number of glial cells which was twice as many a normal brain possessed!! Perhaps these glial cells hold the key to what elevates certain humans to genius.

There are three major types of glial cells in the mature Central Nervous System (CNS):

- **Astrocytes:** Astrocytes have numerous projections that anchor neurons to their blood supply and hence forming the blood brain barrier. They regulate the external chemical environment of neurons by removing excess ions, the notable one being potassium, and recycling neurotransmitters released during synaptic transmission.

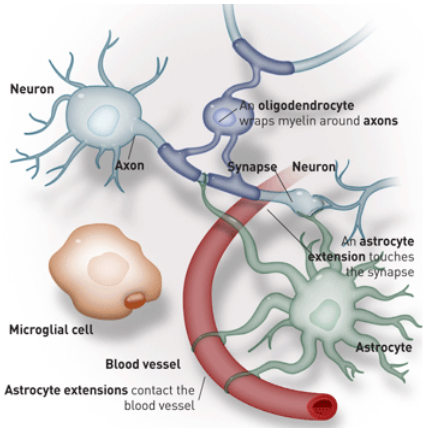

Figure 1.3: The major types of glial cells in the CNS

They also communicate with other types of glia to ultimately ensure smooth signaling in the neuronal network.

- **Oligodendrocytes:** Glial cells in the CNS that are respobsible for producing myelin that insulates axons. Anatomists of earlier centuries called these cells oligodendrocytes which means "short branches" due to their small cell bodies out of which they found several short branches were radiating out. But later, better staining methods revealed that the stubby branches did not end where the old stains failed but rather extended like tentacles of an octopus wrapping around an axon. Each oligodendrocyte can extend its processes to multiple axons and each axon can receive processes from multiple oligodendrocytes.

- **Microglia:** Microglial cells as the name suggests are relatively small with changing shapes and oblong nuclei. In a healthy brain, microglia direct the immune response to brain damage and play an important role in the inflammation that accompanies the damage by multiplying rapidly.

1.5 Oligodendrocytes and Myelination

1.5.1 Myelination

Myelination is the process by which oligodendrocytes (in CNS) ensheathe and electrically insulate axons to facilitate faster conduction of electrical impulses. Myelination occurs throughout childhood and young adulthood and is thought to be completed by the fourth decade of human life when the frontal lobe finishes myelin formation. In interpreting structural alterations and plasticity that the myelinated nerve fibers of the central nervous system exhibit, it is first helpful to understand the normal appearance of myelinated nerve fibers in electron micrographs.

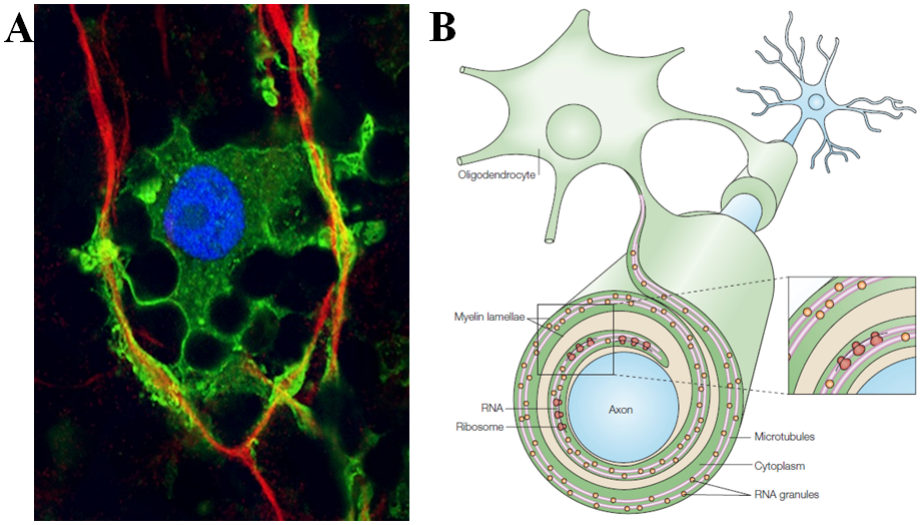

Figure 1.4: **A:** A confocal laser scanning microscopy image of an oligodendrocyte (blue) that extends to form myelin sheaths (green) to encase Purkinje cell axons (red) in the developing rat cerebellum. [*Adapted from http://www.anatsoc.org.uk*] **B:** A diagram depicting how oligodendrocytes (green) wrap myelin around axons (blue) [*Adapted from [1]*]

The myelin sheaths in the central nervous system are formed by a pair of layers of the plasma membrane of the myelin forming oligodendrocyte. The paired plasma membranes wrap around a length of the enclosed axon in a spiral fashion. During development the cytoplasmic surfaces of the paired plasma membrane are separated by oligodendrocyte cytoplasm, but as the sheath matures the cytoplasm is lost and the cytoplasmic surfaces of the plasma membrane become apposed a very compressed intracellular compartment spanning only 30 Å and appears in the electron microscope as a single line, called the major dense line.

Sequential steps in formation of myelin and nodes of Ranvier:

1. Before glial ensheathment, sodium channels are distributed uniformly and at low density.

2. As the axons are ensheathed by glial cells, but before the formation of compact myelin, loose clusters of sodium channels develop at sites that will become nodes

3. Compact myelin is then formed and, as paranodal junctions are established between the myelinating oligodendrocyte and the axon, sodium channels are excluded from the underlying axon membrane and well defined nodal clusters of sodium channels are established.

Not all vertebrate axons are myelinated, but in general, axons larger than 1 micron are myelinated. Recent studies show that the axons provide a signal to the oligodendrocyte

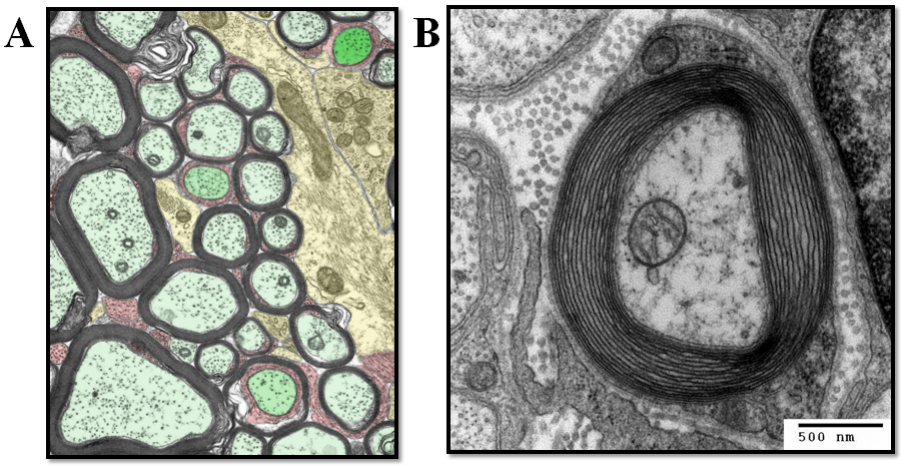

Figure 1.5: **A:** A colored version of an electron micrograph showing the transverse section through the corpus callosum of a 6 year old monkey; Myelinated axons - pale green; astrocytes - yellow: paranodes and nodes - dark green: oligodendrocyte process - red. [*Adapted from http://www.bu.edu/agingbrain/chapter-3-normal-myelinated-nerve-fibers/*] **B:** Transmission electron micrograph of a myelinated axon at a higher magnification [*generated at the Electron Microscopy Facility at Trinity College, Hartford, CT*]

which determine the thickness of the myelin sheath. One important signaling mechanism provided by the axon is via the growth factor neuregulin-1 which binds to ErbB receptor tyrosine kinases expressed by oligodendrocytes. A similar signaling mechanism also exists in Schwann cells. This interaction leads to a defined ratio between axonal diameter and axonal diameter plus myelin sheath, the so-called g-ratio which is usually between 0.6 to 0.7 .

1.5.2 Function of Myelin

In humans, myelination begins in the 14th week of fetal development, although little myelin exists in the brain at the time of birth. During infancy, myelination occurs quickly, leading to a child's fast development, including crawling and walking in the first year.

The main purpose of a myelin layer (or sheath) is to increase the speed at which impulses propagate along the myelinated fiber. Along unmyelinated fibers, impulses move continuously as waves, but, in myelinated fibers, they hop or propagate by saltatory conduction. Myelin decreases capacitance and increases electrical resistance across the cell membrane (the axolemma). Thus, myelination helps prevent the electrical current from leaving the axon, thus functioning as an electrical insulation that increases the conduction velocity and hence decreases the propagation delay.

Chapter 2

Literature Review

The chapter addresses the following through review of the state of art and thus presents the motivation behind the development of the model.

- The necessity for axonal conduction delay as an added dimension to information processing in the brain
- The fact that these delays are not merely fixed values, but rather dynamic adaptive parameters representative of activity dependent plasticity and experimental evidences to prove the same.
- The various mechanisms that could be underpinning adaptive myelination and especially how electrical impulses and their timings hold relevance to myelin plasticity.
- Developing an algorithm to train these adaptive delays.
- Motion perception as an ideal tool to assess the usefulness of the algorithm to model and study adaptive myelination.
- Significance of myelin plasticity on a larger scale.

2.1 Axonal conduction delay, an added dimension to information processing in the brain

The exact cause of human intelligence and its variations ranging from extreme mental retardation to giftedness has always been a topic of debate, but this novel dimension to information processing that is being proposed could potentially lead us to the answer. A correlation between intelligence level ("IQ") and nerve Conduction Velocity (CV) has also been demonstrated in normal individuals [5]. By determining the Reaction Time (RT)/ latency [time from a visual stimulus - checker board pattern reversal - to arrival of an evoked potential at the scalp over the primary cortex], a correlation that had been found

between RT-IQ and the speed of information processing was interpreted as one of the factors determining the level of intelligence and the brain CV was inferred to be the factor affecting this "mental speed".

Typically computational models of neuronal network ignore conduction delays and consider the synaptic weights as the primary set of parameters that hold the key to what the network accomplishes. Challenging this traditional dogma, there has been a growing theoretical interest to consider axonal conduction delays as additional variables to influence the functioning of neural circuits in the brain. In a simulation of a network of cortical spiking neurons [2] conduction delays were kept as fixed parameters and it was shown that synchronous firing in the pre synaptic side is not always effective in eliciting a potent post synaptic response since the spikes arrive at different times in the post synaptic side. Hence, to maximize the post synaptic response the pre synaptic neurons must fire in a temporal pattern determined by the conduction delays as seen in Figure 2.1. Since the firing of these pre synaptic neurons are not synchronous but time-locked to each other, such groups are referred to as "polychronous" and the simultaneous spiking at the post synaptic side is referred to as "isochronicity".

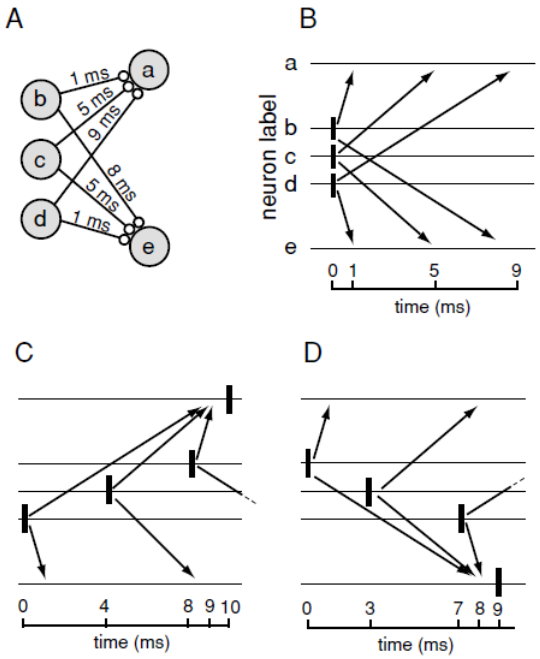

Figure 2.1: **A:** Synaptic connections from neurons b, c, and d to neurons a and e have different fixed axonal conduction delays.**B:** Synchronous firing is not effective in eliciting a potent post synaptic response (vertical bar denotes firing). **C& D:** Different optimal spiking patterns excite different post synaptic neurons [*Adapted from [2]*]

There are various axonal factors that are crucial to establishing a proper speed of con-

duction and hence a proper conduction delay: The thickness of myelin, axon diameter, and the spacing and width of nodes of Ranvier (again controlled by myelination). The two principle mechanisms for changing conduction velocity are altering axon diameter and myelination (vertebrates) with the latter being the most effective way [3]. It has been shown that the axons of retinal ganglion cells located at different eccentricities within the retina show differences in conduction times that are adjusted by the myelin sheath thickness to ensure simultaneous arrival within millisecond precision [4] and this strategy of accomplishing isochronicity is expected to occur in other neural systems as well.

2.2 Experimental evidences for activity dependent myelin plasticity

It is commonly assumed that the conduction speeds and delays are hardwired at birth or fixed at an early developmental stage that they are assigned a constant value if considered as additional parameters in the network [2]. Synaptic weights are the only set of parameters that are generally trained and memories were always considered to be stored solely as synaptic efficacy. But experience driven brain plasticity exerts its influence beyond the synapse and myelin plasticity provides another cellular mechanism to tune neuronal network functions and complement the established mechanisms of synaptic plasticity [6]. Small changes in myelin sheath thickness relative to the axon diameter ($g\ ratio = axon\ diameter/axon\ diameter + myelin\ sheath\ thickness$) can indeed cause substantial changes in the conduction speed and play a major role in functioning of neural circuits. In addition to affecting conduction velocity, myelin is also known to cause a decrease in the refractory period, enabling transmission of spikes at a higher frequency [7].

Occurrence of activity dependent plasticity of action potential propagation delay, in short "propagation plasticity" has also been experimentally proved to scale upto 4 ms or 40% after minutes and 13 ms or 74 % after hours [8]. Thus, the activity dependent myelin plasticity establishes that the axonal conduction delays are adaptive variables which can be trained. The dynamic nature of cerebral myelin and the conspicuous role that experience plays in modulating the brain's infrastructure through activity dependent myelin plasticity has also been elucidated through various experiments:

2.2.1 A DTI study on humans learning juggling

A longitudinal study was carried out on humans for a 6 week period when they learn a novel visuo-motor skill such as juggling and Diffusion Tensor Imaging (DTI) was used to measure the training related changes in the white matter microstructure [9]. DTI, a powerful Magnetic Resonance Imaging (MRI) technique that noninvasively measures the preferential diffusion of protons of water molecules is sensitive to the hindrance of water diffusion due to local tissue boundaries and Fractional Anisotropy (FA), a DTI derived quantitative measure of the directional dependence of water diffusion, reflects anatomical features of

white matter, such as axon caliber, fiber density and myelination. The structurally altered brain regions were all specialized in accurate bimanual arm movements, grasping, visual tracking in the periphery all of which are crucial for a complex visuo-motor skill such as juggling. Activity dependent myelo-modulation could be the potential mechanism through which the functional properties of white matter are affected by experience.

2.2.2 A correlation between piano practicing and increased myelination

Similarly, a study was conducted on pianists and non-musicians and the one region in the brain where the difference between the two groups was found was the posterior limb of the internal capsule which carries the corticospinal tracts which carry the descending fibers from primary sensorimotor and premotor cortices and are of critical importance for independent finger movements in humans and other primates. It has indeed been proposed that increased myelination, caused by neural activity in fiber tracts during training is one mechanism underlying the observed FA increases and training induced white matter adaptations are likely to be important for the high level performance of mature pianists and that the overall susceptibility of such plasticity is high in the childhood during which a large number of fiber systems used in piano performance would have still not completed their maturation [10].

2.2.3 Hypomyelination of PFC via social isolation

On the other hand, it has also been tested whether depriving adult mice of social contact would reduce the adult Prefrontal cortex (PFC) myelination, a region involved in complex emotional and cognitive behavior, given that neuroimaging studies support the concept of ongoing PFC myelination until the third decade of life. Quantification of myelin thickness relative to axonal diameter (g ratio) revealed statistically significant differences between group-housed ($g = 0.810 \pm 0.01$) and socially isolated ($g = 0.876 \pm 0.01$) mice in PFC [11]. Myelin changes in PFC have also been reported in a wide range of psychiatric illness including schizophrenia, autism, anxiety, depression etc. Models of juvenile social isolation results in myelination changes that indeed mimic conditions related to neurodevelopment disorders and hence partially explain the long term consequences of early childhood experience on the development of psychiatric disorders in adulthood.

In short, sensory deprivation via social isolation results in a decrease in myelination of the prefrontal cortex of mice, and learning a new language or complex motor tasks have been shown to increase the myelin thickness and hence alter white-matter structure within the relevant neural circuits in humans, thus emphasizing the importance of myelin plasticity as an experience driven or activity dependent plasticity crucial to learning complex information processing tasks.

2.3 A review of the mechanisms underlying adaptive myelination

Section 2.1 elucidates the importance of axonal conduction delays for information processing in the brain. Section 2.2 addresses the role of activity dependent myelin plasticity in modifying spike arrival timing and hence establishes the fact that these delays are not constant parameters, but variables that could be trained just like synaptic weights. But then, it raises an important question as to how the local information of temporal mismatch influences the oligodendrocytes to modify the myelination. Figuring out this cellular/molecular mechanism that explains activity dependent myelin plasticity could in turn assist in developing the learning algorithm that the oligodendrocytes could potentially follow to modulate the myelin thickness and hence the axonal conduction delays.

2.3.1 Signaling from axons

The observation that, even in culture, oligodendrocytes myelinate only axons, not dendrites, suggests the existence, at the surface of axons, of a recognition signal that permits their ensheathment by the oligodendrocyte processes. But the story is not complete without answering how the myelinated fibers develop with a structure that permits them to tune their conduction velocity as per the neuronal network functional requirements. The axon probably also participates in the regulation of myelin thickness. Single oligodendrocytes can myelinate several axons with different diameters; rather than forming myelin of a fixed diameter, these oligodendrocytes generally form thicker myelin around the larger axon. This suggests that the axon specifies, in a localized way, the number of myelin lamellae formed by a single oligodendrocyte process [12].

2.3.2 Effect of electrical impulses and their timings

The role of electrical activity on myelin formation has also been investigated using specific neurotoxins and it has been shown that inhibition of electrical activity with the specific Na+ channel blocker tetrodotoxin (TTX) prevents the initiation of myelinogenesis [13]. In addition, with K+ that blocks action potentials by maintaining the cells in a depolarized state, or a-scorpion toxin (a-ScTX), which induces repetitive electrical activity by slowing Na+ channel inactivation, the authors have provided evidence that it is the action potential itself which is responsible for the onset of myelination. These observations are consistent with findings such as delayed myelination of the optic nerve in animals reared in the dark, and highly decreased myelination in the naturally blind cape mole rat, whereas how premature eye opening accelerates myelination in the optic nerve.

Experiments were also performed wherein theta-burst stimulation of the hippocampus, which resembles the in-vivo activity, depolarized the oligodendrocytes to -48mV from a resting potential of -75 mV [14]. In these experiments where the action potential latency

had decreased after depolarizing the oligodendrocyte, the filled axon was observed to pass through a myelinated segment extending from a depolarized oligodendrocyte. The authors speculate that the increase in CV may be due to increase in myelin thickness due to osmotic swelling of the myelin secondary to the transmembrane ion fluxes caused by depolarization.

Further, it has also been proved that the timing and the pattern of electrical impulses regulate myelination. Experiments have also been conducted to determine whether differences in patterns of axonal firing could influence myelination [15]. The authors particularly tested whether myelination is inhibited by a frequency of axonal firing characteristic of firing before the onset of myelination. They also concluded that the results raised the possibility that certain patterns of impulse activity could be inhibitory and that an activity dependent mechanism could be involved for myelination in the CNS.

2.3.3 Sub-cellular events in myelo-modulation

If myelin could preferentially form on electrically active axons, then the electrical activity must regulate the sub cellular events necessary for myelin induction. Both neurotransmitters adenosine 5'-triphosphate (ATP) and glutamate (glu) have been implicated in signaling to Oligodendrocyte Progenitor Cells (OPCs)[16]. Glutamatergic synapses can form transiently between axons and some OPCs and the authors have found that release of glutamate from synaptic vesicles along axons of mouse dorsal root ganglion neurons in culture promotes myelin induction by stimulating formation of cholesterol-rich signaling domains between oligodendrocytes and axons, and increasing local synthesis of the major protein in the myelin sheath, Myelin Basic Protein (MBP). The vesicular release of glu from axons also restricts the mobility of MBP, as would be required to wrap MBP-containing membrane selectively around axons firing action potentials. Electrical activity also causes nonvesicular release of the neurotransmitter ATP from axons through volume-regulated anion channels, and ATP released from axons increases myelin formation by regulating OPC differentiation and expression of myelin proteins.

2.3.4 Source of the new myelin

An open question is the source of the new myelin in the adult CNS, though there are a number of possibilities: It could be generated by newly differentiated oligodendrocytes or mature oligodendrocytes could display sufficient plasticity to respond to axonal signals and generate additional myelin segments. Experiments have been performed to explore both the possibilities. Electrical stimulation of the corticospinal tract at the level of the hindbrain in the adult rat has been shown to promote the proliferation of OPCs within the spinal cord and at least some of these OPCs differentiate into postmitotic oligodendrocytes that go on to myelinate the corticospinal axons [17].

A series of experiments were also performed to determine if impulse activity could influence myelination even at later stages of oligodendrocyte development and a link has

indeed been found between myelination, astrocytes and electrical impulse activity in axons mediated by cytokine leukimia inhibiting factor (LIF) [18]. It was shown that LIF is released by astrocytes in response to ATP liberated from axons firing action potentials, subsequently LIF promotes myelination by mature oligodendrocytes.

2.3.5 An in-vivo optogenetic study

Though the modulation of myelination by neuronal activity has mostly been supported only by in-vitro studies so far, in-vivo optogenetic techniques were used in awake, behaving mice as seen in Figure 2.2 to provide evidence that neuronal activity produces changes in myelin forming cells and hence the myelin sheath thickness [19]. [Optogenetic techniques wherein light is delivered at a distance from the target avoids extensive electrode related tissue damage which might affect the Oligodendrocyte Precursor Cells (OPC) dynamics]. Optogenetic stimulation of cortical layer V projection neurons resulted in robust proliferation of OPCs within the premotor circuit, from the deep layers of the premotor cortex to the subcortical projections through the corpus callosum. Four weeks later, an increase in newly generated oligodendrocytes and increased myelin sheath thickness were found within the stimulated premotor circuit and behavioral testing revealed increased swing speed of the correlate forelimb.

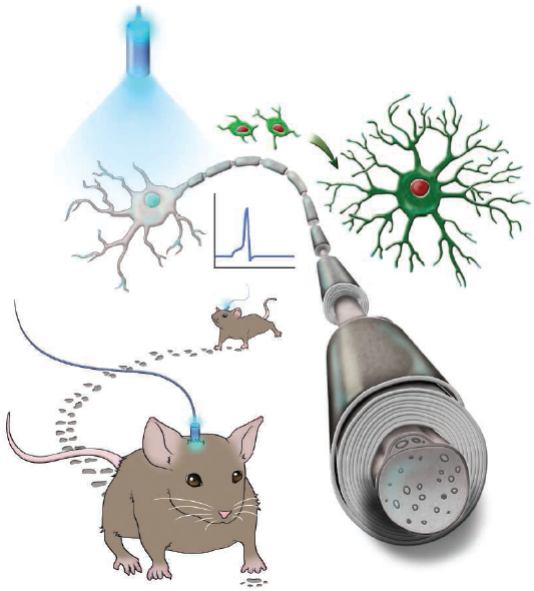

Figure 2.2: An in-vivo optogenetic study on awake mice provided evidence for neuronal impulse activity resulting in increased proliferation of oligodendrocytes and hence increased myelin sheath thickness [*Adapted from [19]*].

2.4 Training the axonal conduction delays

From Section 2.3, it has been made clear that the activity dependent myelination and the events at a cellular level affecting it are all mediated through electrical impulses, their timing and pattern. Moreover, maximizing the speed of conduction is not always what is desired. In some neural systems there is only a need for precise timing of axonal conduction so as to ensure that impulses from multiple input points separated by large distances arrive simultaneously to elicit a spike at the output [20]. For example, while anatomically the cerebellar cortex is deeply folded, from a temporal point of view the olivary neurons function as if they were equidistant from all Purkinje Cells (PCs) in the cerebellar cortex [21]. In other words despite significant differences in the length of individual olivocerebellar axons, the conduction time along them is close to constant and this isochronicity ensures synchrony of Purkinje cell activity with millisecond precision. Hence the best way to model the experience/activity driven plasticity of myelination would be to train the axonal conduction delays in a neuronal network using a spike timing dependent learning rule.

2.4.1 From Hebbian rule to STDP

Hebbian theory describes a basic mechanism for synaptic plasticity, where an increase in synaptic efficacy arises from the presynaptic cell's repeated and persistent stimulation of the postsynaptic cell. The theory is often summarized as "Cells that fire together, wire together". But actually, to take part in firing the post-synaptic neuron, the pre-synaptic neuron should fire just before. Hence STDP is just a temporally asymmetric form of Hebbian learning induced by tight temporal correlations between the spikes of pre- and postsynaptic neurons.

In the STDP process, if an input spike to a neuron occurs immediately before that neuron's output spike, then that input is made stronger. On the other hand, if the input spike to a neuron occurs after its output spike, then it is an acausal case and that input wouldn't have played a role in the generation of the output spike and hence, that synaptic strength is made weaker. Figure 2.3 illustrates the STDP function which shows the change of synaptic weight as a function of relative timing of post and pre synaptic spikes.

Thus the inputs that might be the cause of the post-synaptic neuron's excitation are made even more likely and those which might not be the cause are made less likely to contribute in future. The process continues until only a subset of initial set of connections remain, while the influence of all others is reduced to zero. The ultimate subset of inputs that remain are those that tend to be well correlated in time.

2.4.2 LTP & LTD

With STDP, repeated presynaptic spike arrival a few milliseconds before postsynaptic action potentials leads in many synapse types to long-term potentiation (LTP) of the

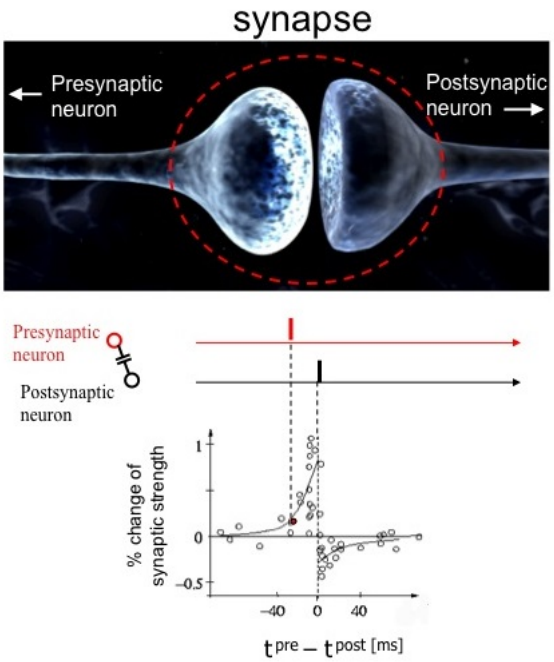

Figure 2.3: The STDP Function (Learning Window)

synapses, whereas repeated spike arrival after postsynaptic spikes leads to long-term depression (LTD) of the same synapse as depicted in Fig 2.4.

The long lasting increase in synaptic strength or "potentiation" is the major cellular mechanism underlying learning or memory. And LTD is one of the several processes that selectively weaken specific synapses in order to make constructive use of synaptic strengthening caused by LTP, because if allowed continuous increase in strength, then the synapses would reach a ceiling level of efficiency which would inhibit encoding of new information.

The cellular mechanism underlying LTP and LTD are as follows: NMDA (N-Methyl D-asparate) receptors detect the coincidence of glutamate release due to pre-synaptic spike and the depolarization due to post synaptic spike and result in the supra-linear rise in post synaptic calcium during LTP. But this requires that an action potential back propagates from the initiation zone near the axon hillock into the dendritic tree making it all the way into the synapse. And probably the post synaptic NMDA receptors are suppressed during STDP timings inducing LTD.

2.4.3 Spike Timing Dependent Plasticity of axonal conduction delays

It has also been argued that regulating the speed of conduction across long fiber tracts would have a major influence on synaptic response, by coordinating the timing of afferent

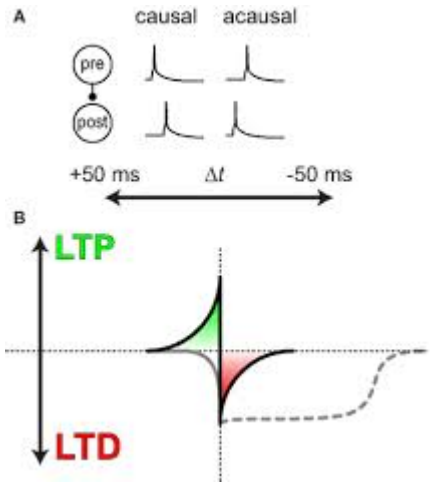

Figure 2.4: Enhancement (LTP) and Reduction (LTD) in synaptic efficacy

input to maximize temporal summation and that the increase in synaptic amplitude could be as large as neurotransmitter-based mechanisms of plasticity, such as Long Term Potentiation (LTP) [22]. Hence we propose that these temporal delays could be trained using the Spike Timing Dependent Plasticity (STDP) kernel, which is a temporally asymmetric variant of Hebbian learning. The idea is to simply fit the axonal conduction delays into the STDP learning window. Training the axonal conduction delay on the presynaptic side using the STDP function depending on the difference in the times the pre and post spikes occur will ultimately ensure isochronicity at the post synaptic side.

2.5 Motion perception as a tool to assess myelo-modulation

Our visual system is able to accurately enable us to perceive spatial and temporal changes in the visual scene as the image moves across the retinal surface, despite a number of sources of variability that can reduce the precision of the spatio-temporal mapping onto central visual areas. Even intuitively perception of motion, for the highly dynamic visual function it is, qualifies as a tool to assess adaptive myelination. Additionally, there are experimental and clinical evidences for the relevance of myelin plasticity in accomplishing the perception of motion and its direction as illustrated below. Hence in our model, we have used perception of motion of bars of different orientations in directions perpendicular to their orientations to study the adaptive myelination.

2.5.1 Adaptation of conduction delays in retinal ganglion axons

The axons of retinal ganglion cells comprise of two segments: Unmyelinated ones as they course across the retina from the cell soma to to the optic disk and myelinated segments as they leave the retina to form the optic nerve. Conduction velocity is much slower in the unmyelinated intra-retinal segment compared to the myelinated extra-retinal one. But it

has been found that there is a strong negative correlation between the intra-retinal and extra-retinal conduction time for axons of individual ganglion cells of X-cell class as seen in Figure 2.5. The net effect was to produce a nearly constant total transmission time between the soma of the retinal X-cell and its central target site and hence time-locked signals at the central target site. Thus the variations in the conduction velocities and hence the axonal propagation time of the retinal ganglion axons ensure that, regardless of the constraints induced by the retinal topography, a precise spatio-temporal central representation of the retinal image is maintained [4].

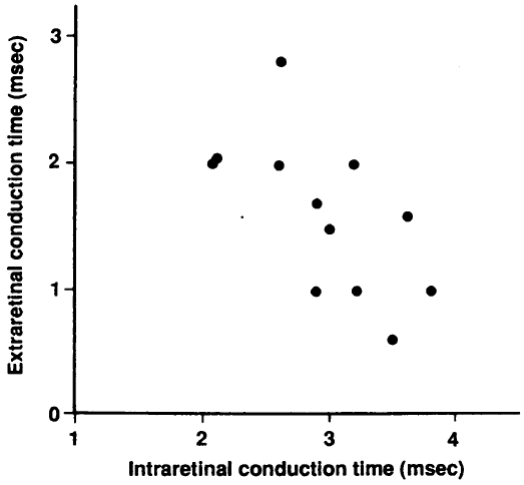

Figure 2.5: Strong negative correlation between the intra-retinal (unmyelinated) and extra-retinal (myelinated) conduction time for the same retinal ganglion X-cell axons, the result of which is a constant total transmission time and hence isochronicity [*Adapted from [4]*].

2.5.2 An Optic Neuritis study

In a study, patients with acute Optic Neuritis (ON), a demyelinating disease of the optic nerve were studied and dynamic visual functions such as motion perception and Visually Evoked Potentials (VEPs) were assessed repeatedly [23]. Their results demonstrated a close correlation between motion perception deficit and prolonged VEP latency, which is believed to reflect the demyelination of optic nerve fibers. Conduction velocity in the visual pathway correlated closely with dynamic visual functions, implicating a need for rapid and isochronous transmission of visual input to perceive motion. Motion perception level may hence serve as a tool to assess the magnitude of myelination in the visual pathways.

2.6 Significance of myelin plasticity

Traditionally learning and plasticity in a neuronal network is associated only with synaptic weights as far as computational models are concerned. Though it defies the reality,

this extreme simplification reduces the computational complexity and at the same time works well especially in accomplishing all functions that are static in nature. But taking into account the supplementary dimension to information processing that we have introduced, helps in modeling highly dynamic networks. Now that it has been established that myelination is no simple electrical insulation but rather an exquisite way of controlling the dynamics of complex information processing in our brain, the model is also inching one step closer to a more neurobiologically realistic representation of our brain function. Additionally understanding myelination and its plasticity is underpinning the treatment of demyelinating diseases and various other cognitive disorders as elaborated below.

2.6.1 Treating diseases of myelin

Adaptive changes in myelin forming cells and myelin sheath thickness and thereby the conduction velocity represent a type of behaviorally relevant neural plasticity that could indeed be leveraged for interventions in diseases of myelin. Human diseases such as Multiple Sclerosis (MS) and inherited leukodystrophies in which the integrity of myelin sheath is lost, make the importance of myelin for CNS functioning all the more apparent. Given that recent studies are demonstrating an unprecedented level of myelin plasticity in the adult CNS, identifying the mechanism that promotes or inhibits myelination during development could aid in the goal of developing novel strategies to promote repair in the demyelinated CNS. Especially if impulse activity could influence myelination even at later stages of oligodendrocyte development, this could have immense relevance to treating demyelinating diseases. Computational models of neuronal networks that learn temporal delays is the first step towards modeling adaptive myelination and consequently way to explore the various parameters that influence myelin plasticity that could of relevance to treating diseases of myelin.

2.6.2 Effects on brain rhythms

The importance of myelin plasticity as an activity dependent plasticity also matters a lot to complex information processing tasks that involve coupling and synchrony among different brain rhythms of various frequencies which have been associated with selective attention, sleep, memory formation, emotion, and consciousness. It has been suggested that even small changes in Conduction Velocity (CV) resulting from subtle changes in myelination and nodal structure will have major effects on oscillatory phenomena, their interference and coupling [3]. Disruption in brain synchronization contributes to autism by destroying the coherence of brain rhythms and slowing overall cognitive processing speed. Thalamocortical dysrhythmia is associated with schizophrenia, obsessive compulsive disorder, and depressive disorder, and the natural frequency of oscillations in the prefrontal cortex are slower in individuals with schizophrenia.

Chapter 3

Methods, Results and Discussions

This chapter is organized as follows:

- A simplified unit with three axonal branches and one post-synaptic neuron is considered and the delays are initially kept as fixed parameters and the time pattern with which the pre-synaptic neurons must fire in order to maximize the post-synaptic response is characterized
- This characterization is generalized to any number of input lines preceding the post-synaptic neuron
- Subsequently an algorithm is proposed to train the conduction delays in the axons of the simplified unit and the process involved in implementing the algorithm and training the delays are discussed in detail
- Finally a complete network of three layers is simulated to achieve motion perception, a dynamic visual function that could be used to assess myelin plasticity and the usefulness of the algorithm is tested by applying it to train the delays in the network

3.1 Input time pattern characterization

The objective is to characterize the pattern of the arrival time of the impulses at the input lines that would give rise to a high output response with the conduction delays in the input lines, synaptic weights and threshold of the post synaptic neuron as network parameters. The response is considered to be the amplitude of the summed PSPs and with a given threshold, the response is analyzed for various time patterns.

A three input line network is simulated and with time at one branch as reference, the response is plotted for varying impulse arrival times at the other two branches. A theoretical analysis is also done to explain how close spikes must occur to result in high output response.

3.1.1 A simplified unit

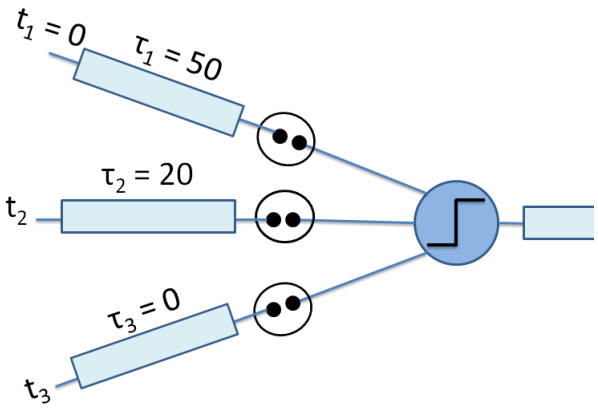

Figure 3.1: A simplified unit with the major parameters

The network as seen in Figure 3.1 has impulses arriving from axons of three neurons as inputs and one neuron at the output. The objective is to figure out the patterns of arrival time vector $[t_1\ t_2\ t_3]$ that results in a sufficiently high amplitude PSP which could result in an impulse at the output depending on threshold. The following are fixed parameters of the network:

- *Delay Vector:* $\tau_1 = 50,\ \tau_2 = 20,\ \tau_3 = 0$
- *Weight Vector:* The synaptic weights determine if there is an EPSP/IPSP at the post synaptic side. In the current context, we have assumed unit positive weight at all the synapses.
- *Threshold at the soma:* The threshold at the soma determines the number of time patterns that give an impulse at the output.
- *Constraints on the time pattern:* We have assumed the arrival time of the input impulse at the first axon to be 0. All the possible arrival times with respect to this are constrained to be within 0 and 80 msecs.

3.1.2 Results and Analysis

For varying patterns of arrival times t_2 & t_3, we have found the summation of the resulting PSPs from all the three input lines and plotted the amplitude/max of the summed PSP for the varying arrival times as seen in Figure 3.2. Following are the the various possible time patterns that result in an impulse on the post synaptic side for different given thresholds v_{th}:

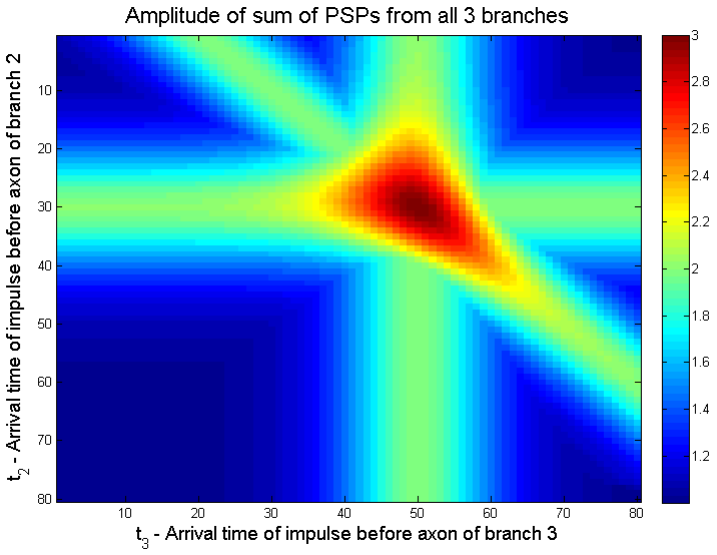

Figure 3.2: Summed PSP variation for different arrival time patterns

Case 1: $2 \leq v_{th} < 3\ V$

There are three input lines and given the fixed delay vector $[\tau_1 = 50,\ \tau_2 = 20,\ \tau_3 = 0]$, there is only one time pattern for which all the PSPs can converge to give the maximum possible amplitude of three. Here, this case occurs for $[t_1 = 0,\ t_2 = 30,\ t_3 = 50]$. This can be seen in the Figure 3.2 as the red spot.

Case 2: $v_{th} < 2\ V$

Out of the 3 branches if PSPs from any two converge, we will get an amplitude of 2 for the summed PSP. Hence there are 3 kinds of patterns which appear as green lines in the Figure 3.2:

- t_3 can be anything and $t_2 = 30$ in which case PSPs from the first two branches will coincide perfectly to give amplitude 2 and above.
- t_2 can be anything and $t_3 = 50$ in which case PSPs from the first and third branches will coincide perfectly to give amplitude 2 and above.
- $t_3 - t_2 = 20$ in which case the arrival times and the delays of the branches 2 and 3 add up accordingly such that the resulting PSPs coincide exactly to give amplitude 2 and above.

Depending on the threshold, the output neuron responds to just one arrival time pattern or multiple kinds of patterns. For example if the threshold is as high as 2.9 then only a 3×4 array of times t_2 & t_3 (out of the 50×50 possibilities) will give a response at the output.

3.1.3 Extrapolation of Results to a simplified unit with any number of branches

The results can be extended to a generic case where there are n input lines, (i.e) impulses arriving from axons of n neurons as input and one neuron at the output. The amplitude of summation of PSPs and the pattern the amplitude will take can be understood by the following way:

There can be various levels of amplitudes. If PSPs from atleast two branches coincide, the amplitude is 2 and the maximum amplitude is n when PSPs from all the n branches coincide. There are $\binom{n}{r}$ ways in which PSPs from r branches out of the n coincide and there will be those many hyper planes with amplitude r. The total number of such hyper planes is:

$$\binom{n}{2} + \binom{n}{3} + ... + \binom{n}{n} = 2^n - n - 1 \tag{3.1}$$

3.1.4 Theoretical Analysis

Here, we theoretically analyze how close two post synaptic spikes should occur so that the second one increases the amplitude of the existing summed PSP amplitude.

Let PSPs occur at times $\xi_i = t_i + \tau_i$ and decay exponentially with time constant κ which is a constant for all PSPs. If the PSPs are added to an existing variable "summed psp" as and when they occur, there would be peaks only at $\xi_i \ \forall \ i = 0, 1, 2, 3...$ Let those peaks be $A_i \ \forall \ i = 0, 1, 2, 3...$ Assuming $A_0 = 1$, $A_i \ \forall \ i = 1, 2, 3...$ can be computed recursively and a closed form expression can be obtained as follows. Note that the subscripts do not denote the number of the branch. It is ordered according to the time at which a PSP occurs.

$$\begin{aligned}
A_1 &= A_0 e^{-(\xi_1 - \xi_0)/\kappa} + 1 \\
&= e^{-(\xi_1 - \xi_0)/\kappa} + 1 \\
A_2 &= A_1 e^{-(\xi_2 - \xi_1)/\kappa} + 1 \\
&= (e^{-(\xi_1 - \xi_0)/\kappa} + 1) e^{-(\xi_2 - \xi_1)/\kappa} + 1 \\
&= e^{-(\xi_2 - \xi_0)/\kappa} + e^{-(\xi_2 - \xi_1)/\kappa} + 1 \\
&... \\
&... \\
A_i &= e^{-(\xi_i - \xi_0)/\kappa} + e^{-(\xi_i - \xi_1)/\kappa} + e^{-(\xi_i - \xi_2)/\kappa} + ... + e^{-(\xi_i - \xi_{i-1})/\kappa} + 1
\end{aligned}$$

Now, at some time instant if I want the next PSP to cause an increase in the amplitude of the PSP_ Sum (i.e), $A_{i+1} > A_i$ then the following condition must be satisfied:

$$\begin{aligned} A_i e^{-(\xi_{i+1}-\xi_i)/\kappa} + 1 &> A_i \\ \Rightarrow e^{-(\xi_{i+1}-\xi_i)/\kappa} &> \frac{A_i - 1}{A_i} \\ \Rightarrow (\xi_{i+1} - \xi_i) &< \kappa \ln(\frac{A_i}{A_i - 1}) \end{aligned}$$

So, we get a relationship for how close two post synaptic spikes must occur so that the second one increases the amplitude of the existing summed PSP.

Now, consider the case where there are totally n branches and there is one spike from each branch leading to a PSP. If n-1 PSPs occur at the same time (i.e), $\xi_1 = \xi_2 = ... = \xi_{n-1}$ (Without loss of generality, assume $\xi_1 = 0$) and just one PSP occurs at a later time (ξ_n), then we get an amplitude of n-1 or above. And there are $\binom{n}{1} = n$ ways this situation could occur. In this case, the following analysis gives a condition for how close the last spike must be to result in an amplitude that is more than n-1.

$$\begin{aligned} A_{n-1} &= n - 1 \\ A_n &= A_{n-1} e^{-(\xi_n - \xi_{n-1})/\kappa} + 1 \\ &= (n-1) e^{-\xi_n/\kappa} + 1 \end{aligned}$$

$$\begin{aligned} Now,\ if\ A_n &> An - 1 \\ \Rightarrow A_{n-1} e^{-\xi_n/\kappa} + 1 &> A_{n-1} \\ \Rightarrow e^{-\xi_n/\kappa} &> \frac{A_{n-1} - 1}{A_{n-1}} \\ \Rightarrow \xi_n &< \kappa \ln(\frac{A_{n-1}}{A_{n-1} - 1}) \\ \Rightarrow \xi_n &< \kappa \ln(\frac{n-1}{n-2}) \end{aligned}$$

For example, consider the case when there are 3 branches (n=3). Consider the situation when $\xi_1 = \xi_2$. The minimum amplitude is 2 which could occur in 3 ways when spikes from any 2 of the 3 branches coincide. The analysis done above could be used to determine how close the third spike must be so that the net PSP has an amplitude that is more than 2. Substituting $A_2 = 2$, we get:

$$\xi_3 < \kappa \ln(2)$$

3.2 Training conduction delays in a network

3.2.1 Spike Timing Dependent Myelin Plasticity (STDMP)

In order to train the conduction delays, we have used an algorithm that is depended on impulse timings. Spike timing dependent plasticity (STDP) algorithm is typically used to adjust the synaptic strength between neurons based on the relative timing of a particular neuron's output and input action potentials. Here the idea is to fit the axonal conduction delays into the standard STDP kernel/Learning window.

3.2.2 STDMP Implementation

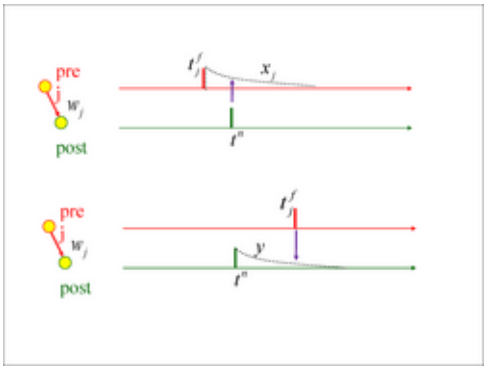

Figure 3.3: Implementation using local variables (traces)

Figure 3.3 represents a method of implementing STDMP using local variables as follows: Pre-synaptic spike leaves a trace $x(t)$ read out at the moment of post synaptic spike and a post synaptic spike also leaves out a trace $y(t)$ read out at the moment of the pre synaptic spike. This trace $y(t)$ could be interpreted as the voltage at the synapse caused by a back-propagating AP or by calcium entry due to a back-propagating AP.

We assume that the conduction delay τ caused by the myelinating glia increases at the moment of post synaptic firing by an amount proportional to the value of trace x(t) left by the presynaptic spike and decreases at the moment of pre-synaptic spike by an amount proportional to the trace y(t) left by the previous post synaptic axonal spike:

$$\frac{d\tau}{dt} = A_+ x(t) \sum_n \delta(t - t_{post}) - A_- y(t) \sum_f \delta(t - t_{pre}) \tag{3.2}$$

where $t_{pre} = t_{ah} + \tau$. In the above equation t_{pre} refers to the time, the impulse arrives just before the synapse, t_{ah} refers to the time, the impulse starts at the axon hillock before passing through the delay line and t_{post} refers to the time, the post synaptic axonal spike occurs.

Thus, if the pre synaptic spike occurs before the post synaptic spike, the axonal conduction delay will increase, resulting in a scenario similar to LTP as seen in Figure 3.4. Similarly, if the post synaptic spike occurs before pre synaptic spike, the conduction delay decreases, resulting in a scenario similar to LTD as seen in Figure 3.5 and eventually the two spikes tend to occur at the same time. This indicates convergence for the STDP algorithm.

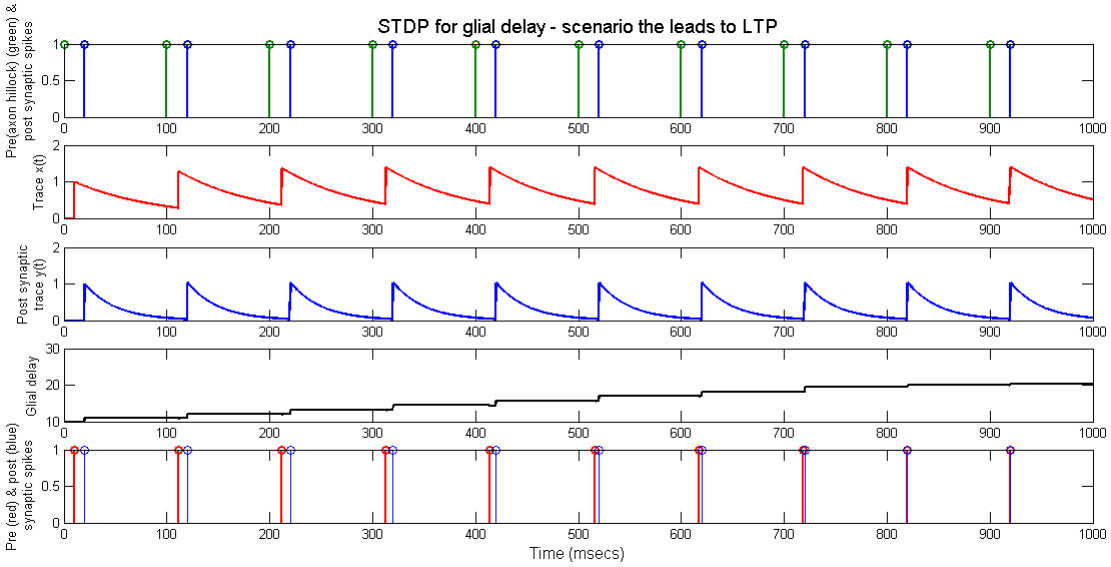

Figure 3.4: STDP to train conduction delays in a scenario similar to LTP

3.2.3 A simplified unit to train conduction delays

Figure 3.6 shows the model of the network implemented. Here I have considered as input impulses from axons of three incoming neurons and a single neuron at the output. The objective is to train the conduction delays caused by the myelin sheaths on the axons which serve as the input lines to each of the dendritic branches of the output neuron in an unsupervised manner to attain the optimum arrival time of post synaptic spikes at the soma of the output neuron.

3.2.4 Process involved in training the delays

There are several batches of training of the delays each spanning consecutive 100 msecs in time. Initially the delays in each input axon is initialized to zero and it is updated in every iteration. The pre synaptic side is stimulated in every batch of the training. The time the pre synaptic AP occurs in every iteration is the delay added to the initialized value relative to that 100 msecs. The number of batches or iterations is decided based on when the pre synaptic spikes converge together to give an impulse of very high strength. Each iteration comprises of the following processes:

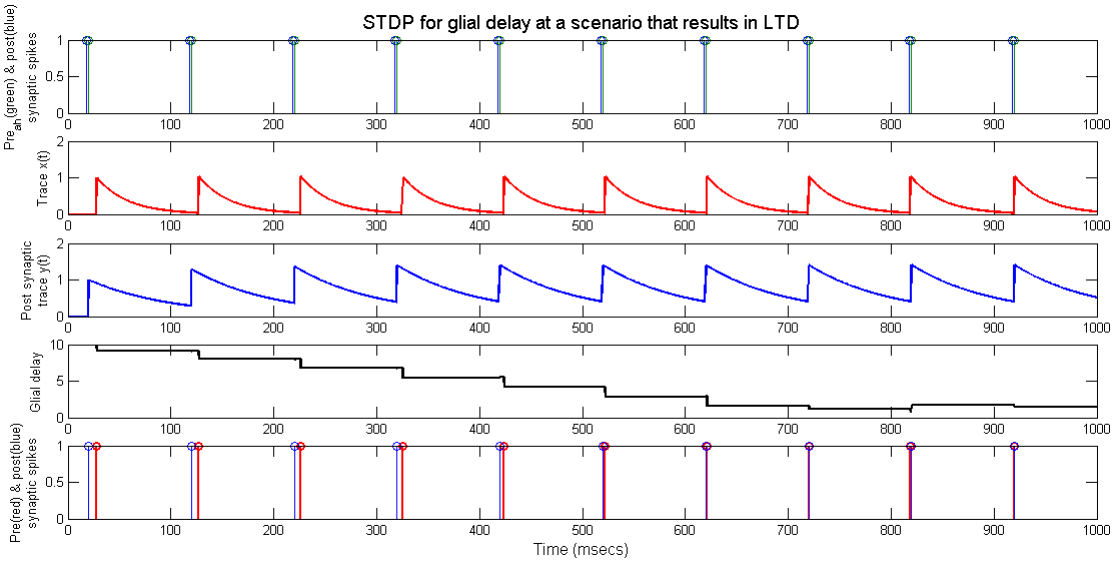

Figure 3.5: STDP to train conduction delays in a scenario similar to LTD

3.2.5 Obtaining PSPs and summation at the soma

The pre synaptic AP at each branch gives rise to a PSP which could be excitatory or inhibitory depending on the synaptic weight. I have assumed unit weight at all the synapses. As depicted in Figure 3.7 the PSP is obtained using the alpha function defined below. Figure 3.8 illustrates the summation of the various PSPs from different dendrites happening at the soma of the output neuron.

$$\alpha(t) = W.[\frac{t-t_0}{\tau}].e^{1-[\frac{t-t_0}{\tau}]},\ t > t_0 \ and\ 0\ otherwise \tag{3.3}$$

3.2.6 Dynamic Threshold

The summed PSP is fed as the input current to a Leaky Integrate and Fire neuron (LIF) and to determine when its membrane potential must be reset, a threshold is updated in every iteration. Initially the threshold is kept zero so that there is an AP at every point even if the PSP is very small in magnitude. This would ensure that there are enough number of changes in delay in the first iteration owing to STDMP every time a pre synaptic or a post synaptic AP occurs. As a simplified approach, the threshold is then increased in every new iteration linearly at a constant rate so that the number of post synaptic APs keep decreasing so that the STDP algorithm converges.

3.2.7 STDMP Algorithm

With the pre synaptic and post synaptic APs computed in every iteration as described above, the STDMP rule is applied to obtain the traces for each of the spike and accordingly

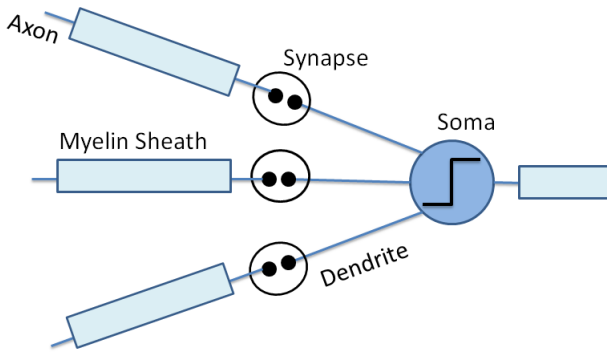

Figure 3.6: The simplified unit used to demonstrate training of conduction delays using STDMP

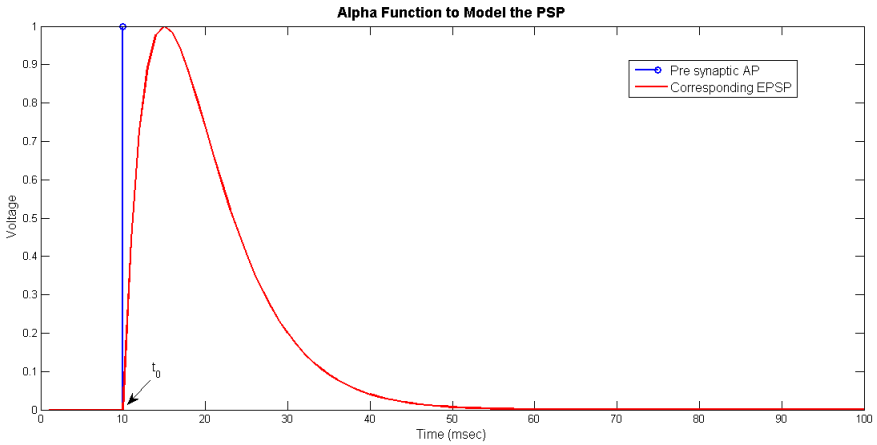

Figure 3.7: Alpha Function to obtain PSP

modulate the conduction delays. The updated delay is used to change the pre synaptic spike time in the next batch of training. Coefficients that modulate the rate of increase and decrease in delay (A_+ & A_- *in Equation* 3.2) are important parameters that determine whether there is a net increase or decrease in delay at the end of all batches of training.

3.2.8 STDMP Results

Figure 3.9 shows the results of STDMP rule applied to all the three input lines to modulate the delays over 8 batches of training each spanning 100 msecs. It can be seen that at the end of the training, the delays decrease in certain lines and increase in other lines.

Figure 3.10 shows the pre synaptic and post synaptic APs over the various batches of training. As mentioned before, the threshold is dynamically adjusted to ensure that initially there are a large number of post synaptic APs so that even pre synaptic spikes

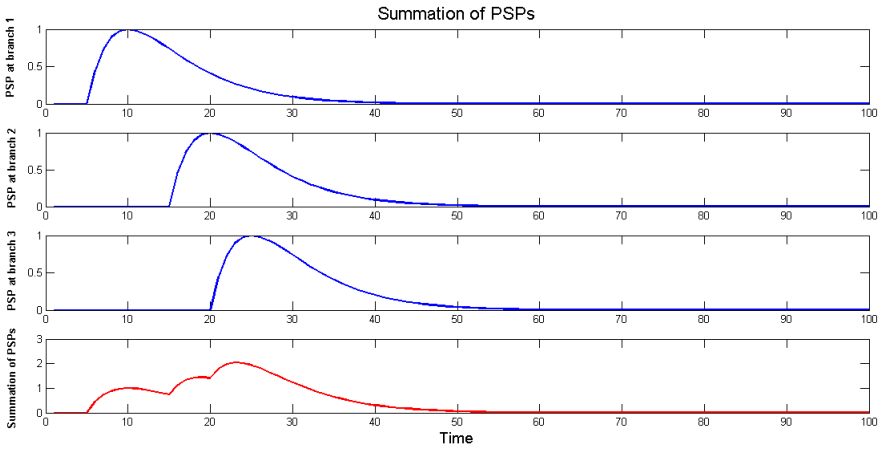

Figure 3.8: Summation of PSPs from different dendrites at the soma

which are initially placed very far off could also be accommodated for training of the delays. Eventually as the threshold increases, it can be seen that the number of post synaptic spikes decreases and the pre synaptic spikes converge.

Figure 3.11 shows the summation of PSPs at each batch of the training and also the linearly increasing threshold levels against which the summed PSP is compared. It can be seen that the amplitude of the summed PSP increases with training since the pre synaptic spikes converge as the conduction delays are accordingly trained.

By training the conduction delays, we have seen how the plasticity of the myelinating glia could affect the arrival time of an input through an axon. In a simple network level we have showed that this could affect the simultaneous arrival of multiple inputs in neural circuits. It can hence be interpreted that the conduction delays increase or decrease (possibly because the myelin sheath thickness decrease or increase) to ensure that there is optimum conduction velocity resulting in isochronicity of impulses for critical information flow.

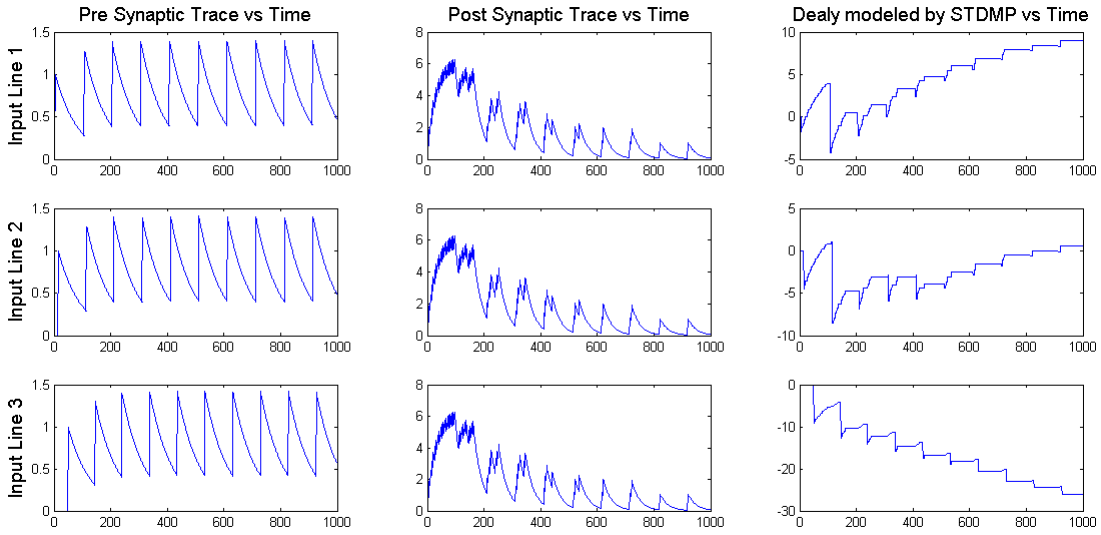

Figure 3.9: STDMP over 8 batches of training each for 100 msecs

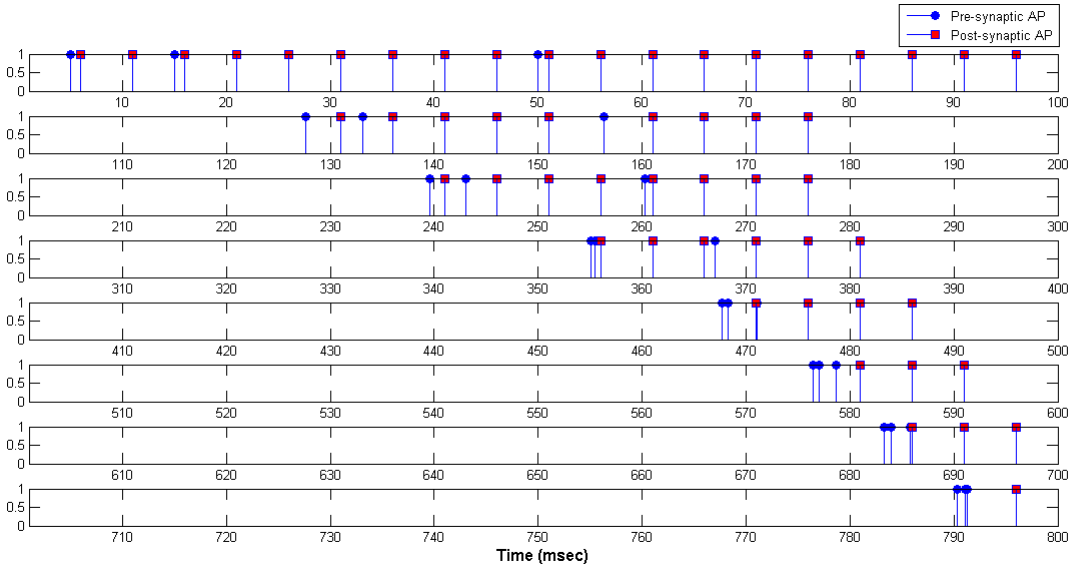

Figure 3.10: Pre synaptic and Post synaptic APs over the batches of training

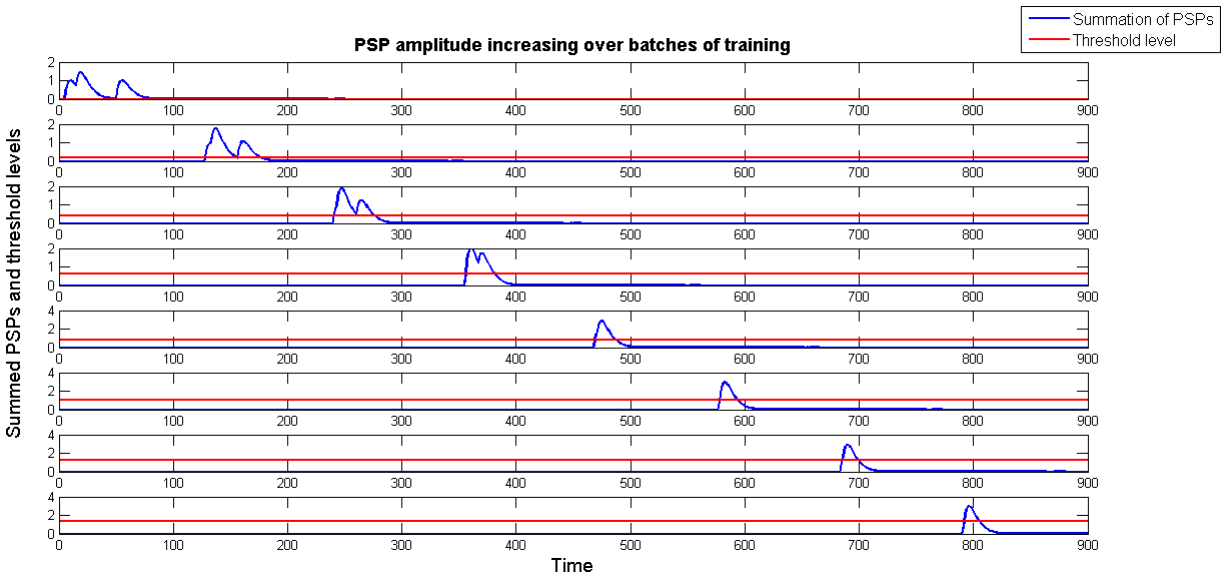

Figure 3.11: Amplitude of the summed PSP increasing with training

3.3 Motion perception model to assess myelin plasticity

3.3.1 Model Overview

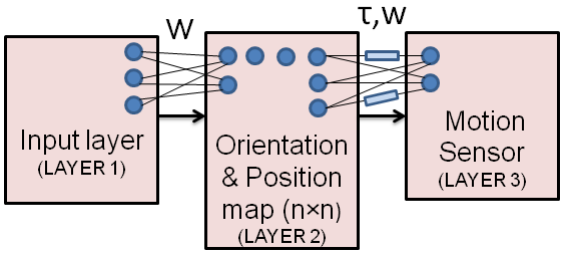

Figure 3.12: Motion Perception Model Architecture

The simulated network consists of three layers as shown in Figure 3.12. The input layer represents different motions of bars of various orientations across the receptive field and the subsequent layer is a 10×10 lattice of neurons wherein a particular neuron maximally responds to a bar of a particular orientation at a particular location on the receptive field. The weights are trained such that the topology is preserved in this transformation of the incoming signal pattern resulting in a Self Organizing Map (SOM). For every bar orientation considered, the various static outputs of SOM for different locations of the bar are cascaded together along with a time stamp as the bar of the particular orientation moves from one location in the receptive field to other. This time varying spike pattern is fed to the third layer which is a 20×1 lattice of Leaky Integrate and Fire (LIF) neurons. The weights and the delays are trained between the second and the third layer. The weights are trained using the hebbian rule and the delays are trained using the proposed STDMP algorithm as elaborated in Section 3.2 and thus different neurons in this output layer are tuned to respond to a unique dynamic spike pattern and hence a unique direction of motion of a bar of a particular orientation. Additionally, since a neighborhood of the winner is trained every time similar to the technique used in a traditional SOM, there is a topological ordering such that for a particular bar orientation, the two directions of motion perpendicular to the orientation always elicit neurons in the neighborhood of each other.

3.3.2 Layer I: Inputs over the receptive field

The layer I represents the input presented to the SOM, which is the motions of bars of different orientations across the receptive field. Four orientations $\theta = 0°, 45°, 90°, 135°$ are considered and the directions of motions are presumed to be only perpendicular to the bar orientation. Hence, there are eight cases of bar motions in all as seen in Figure 3.13.

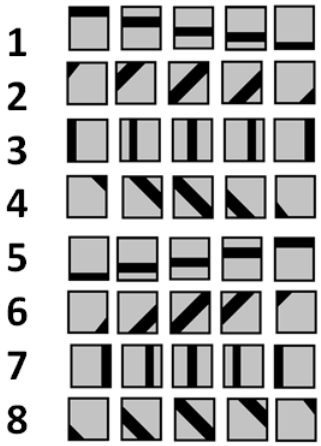

Figure 3.13: Cases 1-8 depicting the bars of different orientations and their directions of motion with time

3.3.3 Layer II: Self Organizing Map

A bar of a particular orientation at a particular location in the receptive field is taken as one input fed to the SOM. The output lattice here is a 10×10 2D lattice and one neuron in the lattice maximally responds to one input. But the principal goal of SOM is to preserve the topological ordering of the incoming signal patterns. In other words, weights would be trained accordingly so that nearby inputs elicit spikes in nearby neurons in the output lattice. Here, the various spatial locations of bars of each orientation are all mapped closely together in the output lattice such that they form separate clusters as illustrated in Figure 3.14.

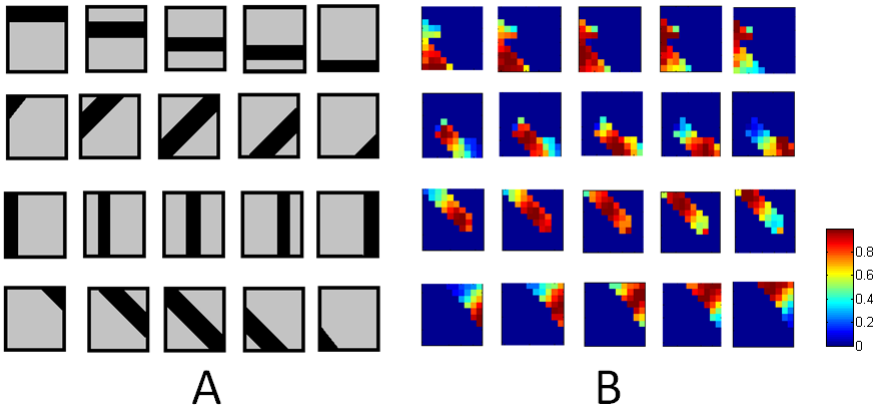

Figure 3.14: Pictorial representation of **(A)** the input patterns and **(B)** the output of the SOM corresponding to each input pattern [The SOM is a 10×10 lattice wherein red denotes the neuron with maximal response and blue the neuron with minimal response for each input pattern]

The algorithm responsible for formation of SOM proceeds first by initializing the synaptic weights in the network. For each input pattern, the neuron whose weight vector has the minimum euclidean distance from the input vector is declared the "winner neuron". The winner neuron is (i^*,j^*) for which $y_{i^*j^*} > y_{ij}\ \forall\ (i,j) \neq (i^*,j^*)$. The winning neuron determines the spatial location of a topological neighborhood of excited neurons, thereby providing the basis for cooperation among such neighboring neurons. As in competitive learning, the weight vector of the winner should be moved closer towards the input x . In addition, the weights of the neurons close to the winner are also moved towards the input but with a lower learning rate that decays exponentially as the distance of the neuron from the winning neuron increases:

$$\triangle w_{i^*j^*} = \eta(x - w_{i^*j^*}) \tag{3.4}$$

$$\triangle w_{ij} = \eta\lambda(i,j,i^*,j^*)(x - w_{ij}) \tag{3.5}$$

where $(i,j) \in N$ where N is the neighborhood that decreases exponentially with time as the training progresses and $\lambda(i,j,i^*,j^*) = exp(-(i-i^*)^2 - (j-j^*)^2)$.

3.3.4 Processing of layer II output

The layer II, self organizing map's response is processed before being fed into the output layer, layer III. Currently we have obtained a separate response from the SOM for every spatial location of the bar on the receptive field. But to perceive motion, we would like to encode the variation in spatial locations over time for every bar orientation. Hence we interpret the input patterns of bars of each orientations as they move across the receptive field to be cascaded one after the other with a time stamp each. The 10×10 SOM is viewed as a 100×1 SOM for simplicity and for each time step, only the neuron that maximally responds is considered to elicit a spike. Figure 3.15 shows the processing for 2 cases of bar motions. It can be seen that for the two directions of motion for a bar of a particular orientation, the spikes elicited in the 100×1 lattice over time is just a mirror image with respect to the time axis. In other words, motion in opposite directions excite the same neurons but in the reverse order with respect to time.

3.3.5 Layer III: Output layer of spiking neurons

Figure 3.16 pictorially demonstrates how the SOM output is processed into dynamic spike trains and subsequently fed to the output layer to train the weights (w) and the delays (τ) between layer II and layer III. Here, unlike the previous layers the delay is a crucial parameter that must be trained in order to encode the dynamics in the neuronal activity. Additionally, to make the network more realistic, this is a layer of spiking neurons.

The eight cases of bar motions and their resultant dynamic spike patterns can also be

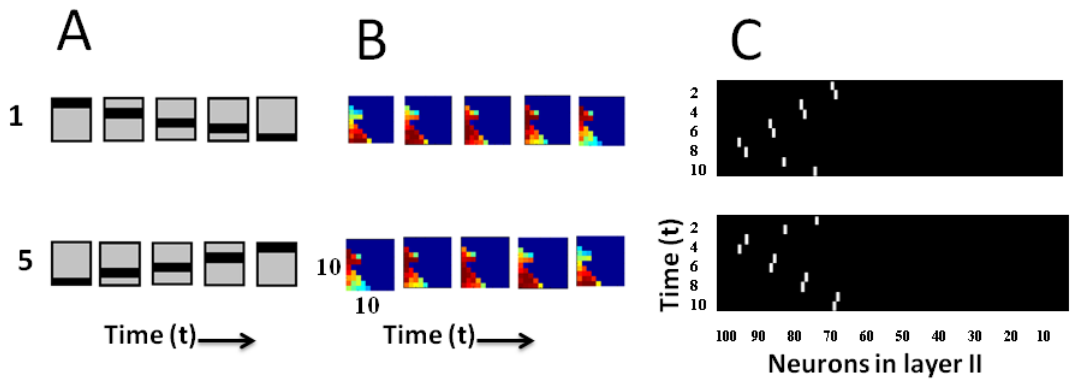

Figure 3.15: **A**: Two directions of motion for a bar oriented at $\theta = 0°$ **B**: Output of the 10×10 SOM corresponding to each input pattern wherein red denotes the neuron with maximal response and blue the neuron with minimal response **C**: Processed layer II output; White bar denotes the spike elicited by the neuron that maximally responds to the input at any given time step

represented as shown in Figure 3.17. Color coding and representing such higher dimensional data in lower dimensions makes visualization easier as it will be seen later. Here for each of the 8 cases, the occurrence of spikes over the ten time steps is captured in one vertical each using the color coding. The weights are trained using hebbian rule unlike the delays which are trained using STDMP. Since the training of conduction delays underpins the entire encoding of the spike dynamics, stringent temporal correlation is necessary, whereas training the weights is merely to suppress the connections from the many neurons in the second layer that are not excited at all. Hence the simple hebbian rule is sufficient to train the weights to achieve the required results. An important point to be noted is that the synaptic weights must be normalized after applying hebb's law:

$$\triangle w_i = \eta.y.x_i \tag{3.6}$$

where

$$y = \sum_{i=1}^{n} w_i x_i \tag{3.7}$$

and normalization is done following that as:

$$w \longleftarrow w/||w|| \tag{3.8}$$

This prevents the weights from growing without bound and constraints the weight vector to be of unit norm. Additionally, it also introduces competition between the input neurons that results in pruning of the unnecessary weights: for one weight to grow, another must shrink. Figure 3.18 **B** shows the synaptic weights from all the neurons in layer II to the corresponding winner neuron in each case. It can be seen that except for the neurons that are excited in layer II, all other neurons have their synaptic efficacy pruned.

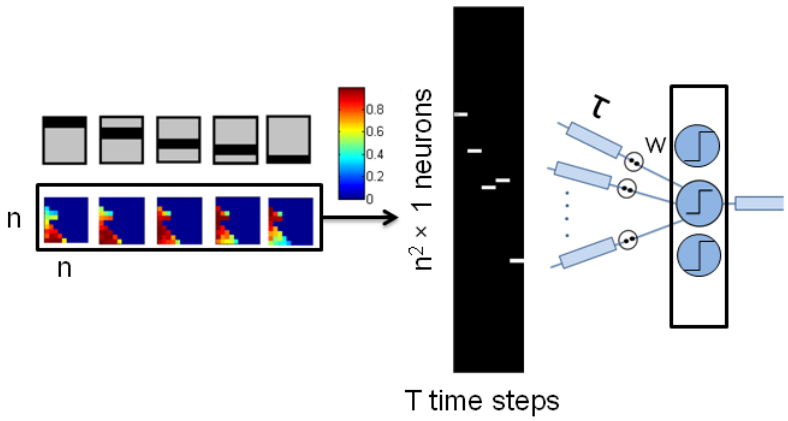

Figure 3.16: Processed second layer output is fed to the third layer to train the delays (τ) and the weights (w)

Furthermore, the delays are simultaneously trained using the STDMP algorithm. The pre synaptic spikes are the dynamic spikes processed from the layer II output, delayed by the initialized values of the axonal conduction delays between layer II and III. PSPs are calculated from these spikes by modeling the synapse using an alpha function with the weights as coefficients. The PSPs are temporally summed at the soma and this is the input current I(t) fed to the LIF neurons of the output layer. The neuron in the output layer for which the integrated PSP sum is maximum is considered as the winner. The post synaptic spikes are subsequently calculated from the membrane potential of the LIF neuron, which is modeled as just a "leaky integrator" of its input I(t):

$$\tau_m \frac{dv}{dt} = -v(t) + RI(t) \tag{3.9}$$

where $v(t)$ denotes the membrane potential at time t, τ_m is the membrane time constant and R is the membrane resistance. The equation describes a simple RC circuit where the leakage term is due to the resistor and the integration of $I(t)$ is due to the capacitor in parallel with the resistor. The spiking event is not explicitly modeled in the above equation. Instead, when the membrane potential $v(t)$ reaches a certain threshold v_{th} (spiking threshold), it is instantaneously reset to a lower value v_r (reset potential) and the leaky integration process starts anew. In this model, the threshold is also dynamic and trained along with the weights and delays in a linear fashion with every epoch of training. As STDP proceeds, the PSP amplitude increases and this would result in more number of post synaptic spikes had threshold been constant and as a result, STDP would never converge. Hence increasing the threshold is necessary.

Figure 3.19 shows the tight correlation between the input spike patterns **(A)** and the trained delays **(B)**. It can be seen that input AP arrival time added with the corresponding delay for every line from the active neurons in layer II would result in the same value implying isochronicity/synchrony at the post synaptic side attained after training. From

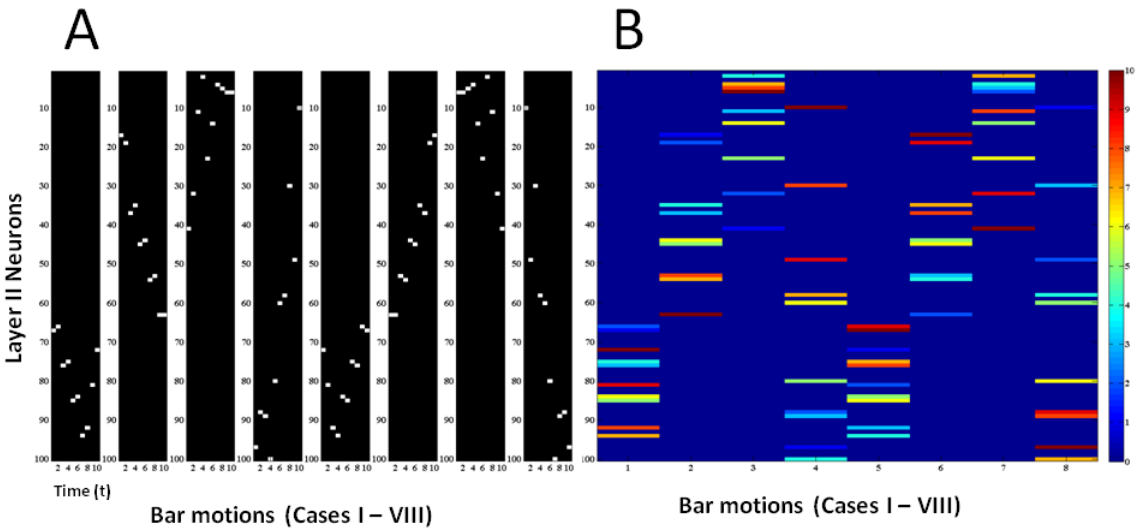

Figure 3.17: **A**: Dynamic spike patterns after processing layer II output **B**: Alternative representation of A using color coding to represent timings of spikes [Blue denotes the neuron that spikes at the first time step and red denotes the neuron which spikes at the last time step]

(B) it can also be noted how the delays are randomly initialized for all lines and owing to STDP, only the delays in the lines where spikes occur are appropriately trained.

Thus for every case of bar motions, a winner having the maximum summed PSP amplitude is identified. Figure 3.20 **(B)** shows the integrated PSP amplitude for the various neurons of the output layer and **(C)** shows the winner alone in each case. Similar to the technique used in training SOMs, the delays of the neighbors of the winners are also trained using STDP in every iteration. Thus, as seen in the figure the integrated PSP amplitude varies gradually around the winner in each case. This results in a topological ordering in the output as it can be seen in **(C)**. The winner neurons of cases I & V, II & V1, III & VII, IV & VIII are always in the neighborhood of each other. In other words, the two directions of motion for bars of every orientation always excite neurons that are adjacent to each other.

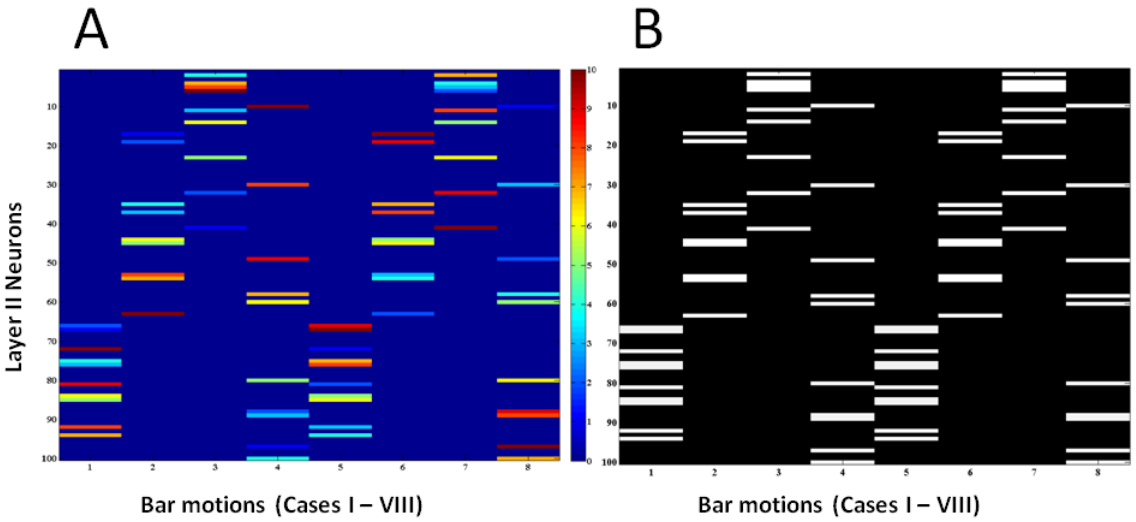

Figure 3.18: **A**: SOM output as dynamic spike patterns whose timings are color coded [Blue denotes the neuron that spikes at the first time step and red denotes the neuron which spikes at the last time step] **B**: Synaptic weights from all neurons in layer II to the corresponding winner neuron for each case of bar motions [black denotes weight = 0 and white tends to a weight of 1]

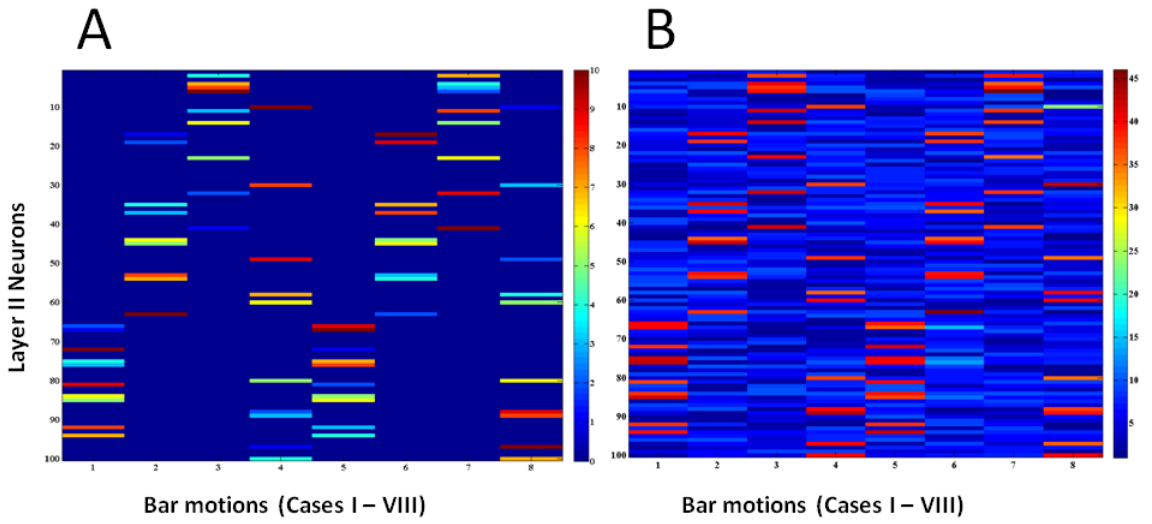

Figure 3.19: **A**: SOM output as dynamic spike patterns whose timings are color coded [Blue denotes the neuron that spikes at the first time step and red denotes the neuron which spikes at the last time step] **B**: Conduction delays in the axons from all neurons in layer II to the corresponding winner neuron for each case of bar motions [color denotes the value of the delay]

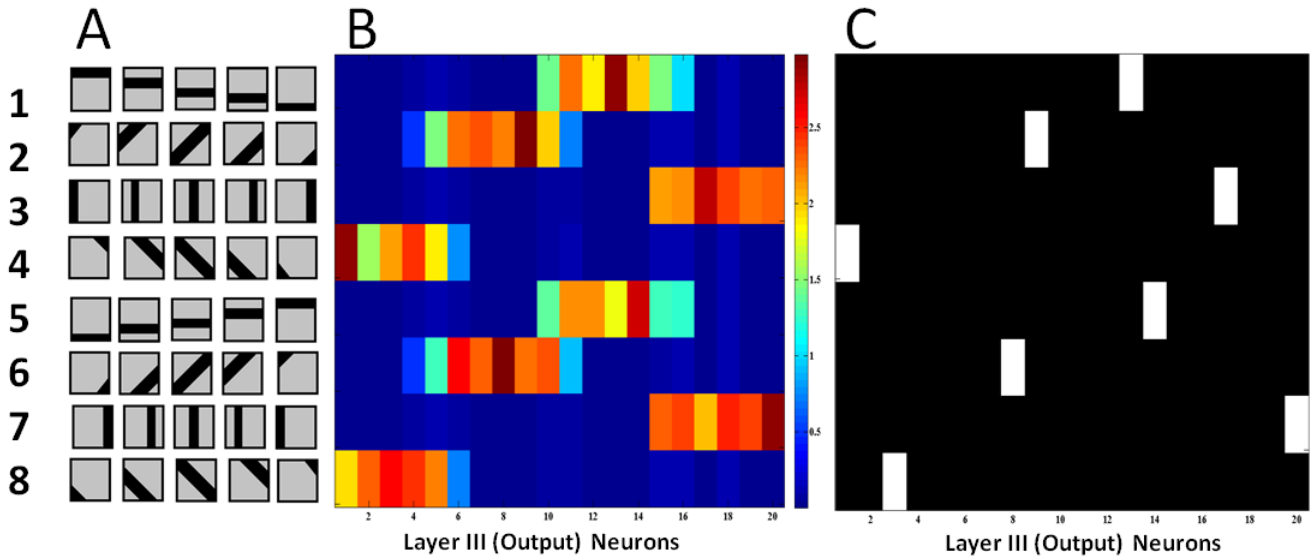

Figure 3.20: **A**: The various cases of bar orientations and directions of motion **B**: Integrated PSP amplitude for every neuron in the output layer for each case **C**: Winner neurons in the output layer which are the neurons with maximum PSP amplitude in each case

Chapter 4

Conclusion

- Until recently, learning and plasticity in the brain has been associated only with synaptic weights. Here, we primarily emphasize the importance of axonal conduction delays as an added dimension to information processing in the brain.

- We have considered simplified units of few axonal branches, a post synaptic neuron and the time pattern of firing of the pre-synaptic neurons that results in maximum post-synaptic response has been characterized computationally and theoretically as shown in Section 3.1

- The review of the state of art has also revealed experimental evidence for the fact that these delays are not merely hard-wired values but time varying variables as seen in Section 2.2. The dynamics of these delays are attributed to the myelin plasticity brought about by the oligodendrocytes, glial cells that are responsible for myelination in the CNS.

- The various mechanisms that could be underpinning adaptive myelination has been reviewed and especially how electrical impulses and their timings hold relevance to myelin plasticity has been analyzed as shown in Section 2.3

- Subsequently we have developed an algorithm as demonstrated in Section 3.2 that is dependent on the spike timings to train the delays. This algorithm is motivated from the traditional STDP algorithm that results in LTP and LTD of the synaptic efficacy.

- Motion perception, a highly dynamic visual function is considered to assess the myelin plasticity. As illustrated in Section 3.3, a three layered network is used to achieve motion perception of bars of various orientations and the algorithm developed is used to train the axonal conduction delays and consequently the usefulness of the algorithm in characterizing adaptive myelination is analyzed.

4.1 Scope and Future Work

- Currently, the motion perception model used to assess myelin plasticity is a three layered network wherein the output layer is a one-dimensional layer of twenty neurons. This layer could be extended into a two-dimensional layer to make it more realistic since a very thin slice of our cerebral cortex can be considered to be two-dimensional.

- Apart from direction sensing, even velocity sensing can be used as a tool to assess the myelin plasticity and the usefulness of the proposed algorithm. The input patterns to be presented to the SOM must be bars of various orientations with different rates of motion.

- The STDMP algorithm that we have proposed here states that the myelin thickness varies on an appropriate time scale depending on the relative pre-post spikes timings. This proposition if experimentally verified could lead us to the answer to the precise molecular mechanisms underlying myelin plasticity which would in-turn aid in development of novel strategies to treat demyelinating disorders.

References

[1] Sherman, Diane L., and Peter J. Brophy. "Mechanisms of axon ensheathment and myelin growth." Nature Reviews Neuroscience 6.9 (2005): 683-690.

[2] Izhikevich, Eugene M. "Polychronization: computation with spikes." Neural computation 18.2 (2006): 245-282.

[3] Pajevic, Sinisa, Peter J. Basser, and R. Douglas Fields. "Role of myelin plasticity in oscillations and synchrony of neuronal activity." Neuroscience 276 (2014): 135-147.

[4] Stanford, L. R. "Conduction velocity variations minimize conduction time differences among retinal ganglion cell axons." Science 238.4825 (1987): 358-360.

[5] Reed, T. Edward, and Arthur R. Jensen. "Conduction velocity in a brain nerve pathway of normal adults correlates with intelligence level." Intelligence 16.3 (1992): 259-272.

[6] Markham, Julie A., and William T. Greenough. "Experience-driven brain plasticity: beyond the synapse." Neuron glia biology 1.04 (2004): 351-363.

[7] Fields, R. Douglas. "White matter in learning, cognition and psychiatric disorders." Trends in neurosciences 31.7 (2008): 361-370.

[8] Bakkum, Douglas J., Zenas C. Chao, and Steve M. Potter. "Long-term activity-dependent plasticity of action potential propagation delay and amplitude in cortical networks." PLOS one 3.5 (2008): e2088.

[9] Scholz, Jan, et al. "Training induces changes in white-matter architecture." Nature neuroscience 12.11 (2009): 1370-1371.

[10] Bengtsson, Sara L., et al. "Extensive piano practicing has regionally specific effects on white matter development." Nature neuroscience 8.9 (2005): 1148-1150.

[11] Liu, Jia, et al. "Impaired adult myelination in the prefrontal cortex of socially isolated mice." Nature neuroscience 15.12 (2012): 1621-1623.

[12] Waxman, Stephen G. "Axon-glia interactions: building a smart nerve fiber." Current Biology 7.7 (1997): R406-R410.

[13] Demerens, C., et al. "Induction of myelination in the central nervous system by electrical activity." Proceedings of the National Academy of Sciences 93.18 (1996): 9887-9892.

[14] Fields, R. Douglas. "Oligodendrocytes changing the rules: action potentials in glia and oligodendrocytes controlling action potentials." The Neuroscientist 14.6 (2008): 540-543.

[15] Stevens, Beth, Sandra Tanner, and R. Douglas Fields. "Control of myelination by specific patterns of neural impulses." The Journal of neuroscience 18.22 (1998): 9303-9311.

[16] Wake, Hiroaki, Philip R. Lee, and R. Douglas Fields. "Control of local protein synthesis and initial events in myelination by action potentials." Science 333.6049 (2011): 1647-1651.

[17] Emery, Ben. "Regulation of oligodendrocyte differentiation and myelination." Science 330.6005 (2010): 779-782.

[18] Ishibashi, Tomoko, et al. "Astrocytes promote myelination in response to electrical impulses." Neuron 49.6 (2006): 823-832.

[19] Gibson, Erin M., et al. "Neuronal activity promotes oligodendrogenesis and adaptive myelination in the mammalian brain." Science 344.6183 (2014): 1252304.

[20] Zalc, Bernard, and R. Douglas Fields. "Do action potentials regulate myelination?." The Neuroscientist 6.1 (2000): 5-13.

[21] Sugihara, I., E. J. Lang, and R. Llinas. "Uniform olivocerebellar conduction time underlies Purkinje cell complex spike synchronicity in the rat cerebellum." The Journal of physiology 470.1 (1993): 243-271.

[22] Fields, R. Douglas. "Myelination: an overlooked mechanism of synaptic plasticity?." The Neuroscientist 11.6 (2005): 528-531.

[23] Raz, Noa, et al. "Demyelination affects temporal aspects of perception: an optic neuritis study." Annals of neurology 71.4 (2012): 531-538.

Appendix

Code for motion perception model: layer II SOM

```
clear all;
inp_cases=40;
%Input to the SOM
[inp,inp_dimn]=input_to_spatial_som(inp_cases);
inp_plot=modify_input_for_plotting(inp);

m_lattice=10;
n_lattice=10;
%initialization of weights
w=initialize_weights(m_lattice,n_lattice,inp_dimn);

etao=5;
do=10;
T=1000;
t=1;

while (t<=T)
    eta=etao*exp(-t/T);%learning rate
    d=round(do*exp(-t/T));%neighborhood
    wstar=zeros(inp_cases,2);
    for i=1:inp_cases
        wstar=find_winner_spatial_som(i,inp,w,m_lattice,n_lattice
            ,inp_dimn,wstar);
        w = train_wts_spatial_som(inp,i,w,wstar,inp_dimn,eta,d,
            m_lattice,n_lattice);
    end
    t=t+1;
end

y = fn_plot(inp_plot,inp,m_lattice,n_lattice,w,inp_dimn,inp_cases
    );
```

```
%Convert the 10*10 2d output lattice stimulation into a sequence of time
%frames of 100*1 points stimulation to feed it into the next layer
inp_2=input_for_next_layer(m_lattice,n_lattice,wstar);
save('inp_2.mat','inp_2');
figure(2);
for i=1:4
subplot(1,4,i);%4 directions of movement
imagesc(inp_2(:,:,i));
end
colormap(gray);
```

Code for motion perception model: output layer

```
clear all;
%The output of the spatial SOM given as input
load('inp_2');
n=length(inp_2);
T=10;
n_op=20;
n_epoch=10;
t_max=50;
eta=0.05;
eta_nbhr=0.02;
d=6;
v_thresh=0.5;
n_cases=80;%Reverse movements for each of the directions
winner = zeros(n_epoch,n_cases);
tau = round(1+rand(n,n_op)*(10-1));
wt = ones(n,n_op);
%Input to train the delays
input = input_to_temporal_map(inp_2,n_cases,n,T);%Just appending the response for reverse movement
figure(1);
for i=1:8
subplot(1,8,i);
imagesc(input(:,:,i*10));
colormap(gray);
end

%Input to train the weights
```

```
27 inp_wt = input_to_train_wts(input,n,T,n_cases);%average over time
       frames
28
29 for epoch=1:n_epoch
30     fprintf('Epoch: %d\n', epoch);
31     pre_trace=zeros(n_op,n);
32     post_trace=zeros(n_op,n);
33     max_psp_sum=zeros(n_cases,n_op);
34     v_thresh=v_thresh+0.1;
35     d=d-2;
36     for train=1:n_cases
37         fprintf('Training Case: %d\n', train);
38         psp_sum = zeros(n_op,t_max);
39
40         input_del=zeros(n,t_max,n_op);
41         for neuron=1:n_op
42             %Delay the inputs by tau's for each line for each
                   neuron
43             input_del = delay_the_input(input_del,train,neuron,
                   input,tau,n,T);
44             %Calculate psps and their summation for each neuron
45             [psp_sum,max_psp_sum] = psp_summation(input_del,wt,n,
                   T,t_max,neuron,psp_sum,max_psp_sum,train);
46         end
47         %Find the winner neuron with the highest psp_sum
               amplitude
48         winner = find_the_winner(max_psp_sum,winner,epoch,train,
               n_op);
49         win=winner(epoch,train);
50         V=lif_neuron(psp_sum,t_max,n_op,v_thresh);
51
52         %Train weights using hebbian to suppress lines with no
               pre spikes
53         y_avg=1;
54         wt(:,win)=wt(:,win)+eta*y_avg*inp_wt(:,train);
55         wt(:,win)=wt(:,win)./norm(wt(:,win));
56         %Train the delays of the winner using STDP
57         tau = stdp_for_winner_lif_neuron(V,pre_trace,post_trace,
               input_del,tau,n,t_max,win);
58
59         jstar=win;
60         for dd=1:d
61             jj=jstar-dd;
```

```
62                 if (jj>=1)
63                     tau = stdp_for_nbhr_lif_neuron(V,pre_trace,
                           post_trace,input_del,tau,n,t_max,jj);
64                     y_avg=1;
65                     wt(:,jj)=wt(:,jj)+eta_nbhr*y_avg*inp_wt(:,train);
66                     wt(:,jj)=wt(:,jj)./norm(wt(:,jj));
67                 end
68
69                 jj=jstar+dd;
70                 if (jj<=n_op)
71                     tau = stdp_for_nbhr_lif_neuron(V,pre_trace,
                           post_trace,input_del,tau,n,t_max,jj);
72                     y_avg=1;
73                     wt(:,jj)=wt(:,jj)+eta_nbhr*y_avg*inp_wt(:,train);
74                     wt(:,jj)=wt(:,jj)./norm(wt(:,jj));
75                 end
76             end
77         end
78 end
79 %Plot time arrival at all the branches for each of the 8 motions
80 time_arrival=zeros(100,8);
81 for k=1:8
82     for i=1:10
83         for j=1:100
84             if input(j,i,k*10)==1
85                 time_arrival(j,k)=i;
86             end
87         end
88     end
89 end
90 figure(2);
91 imagesc(time_arrival);
92 colorbar();
93
94 %Plot corresponding delays
95 tau_fin=zeros(100,8);
96 for i=1:8
97     winn=winner(n_epoch,i*10);
98     tau_fin(:,i)=tau(:,winn);
99 end
100 figure(3);
101 imagesc(tau_fin);
102 colorbar();
```

```
103
104 %Plot corresponding weights
105 wt_fin=zeros(100,8);
106 for i=1:8
107     winn=winner(n_epoch,i*10);
108     wt_fin(:,i)=wt(:,winn);
109 end
110 figure(4);
111 imagesc(wt_fin);
112 colormap(gray);
113
114 %Plot the winner out of the 20 output neurons for each of the 8
    motions
115 winner_final = winner_final_epoch(winner,n_epoch,n_cases,n_op);
116 figure(5);
117 imagesc(winner_final);
118 colormap(gray);
119 xlabel('Output neuron number','fontsize',12);
120 ylabel('Training case number','fontsize',12);
121 title('The winner neuron for each training case','fontsize',14);
122
123 figure(6);
124 imagesc(max_psp_sum);
125 xlabel('Output neuron number','fontsize',12);
126 ylabel('Training case number','fontsize',12);
127 title('The output (max psp sum) for each training case','fontsize
    ',14);
128 colorbar();
```

Code for an STDMP implemtation

```
1 function tau = stdp_for_winner_lif_neuron(V,pre_trace_del,
    post_trace_del,input_del,tau,n,t_max,win)
2
3     xhist = zeros(n,t_max);
4     yhist = zeros(n,t_max);
5     delhist = zeros(n,t_max);
6     [pks,locns]=findpeaks(V(win,:));
7     post_spikes_time=locns./100;
8     dt=1;
9     a=0.65;b=0.65;%This value gives the perfect delay plot
10    for i=1:1:n
11        x=pre_trace_del(win,i);
```

```
12          y=post_trace_del(win,i);
13          del=tau(i,win);
14          for t=1:1:t_max
15              x = x*exp(-dt/80);% tau_{+} = 80
16              y = y*exp(-dt/30);% tau_{-} = 30
17              if(input_del(i,t,win)==1)
18                  x=x+1;
19              end
20              for z = 1:length(post_spikes_time)
21                  post = post_spikes_time(z);
22                  if (t == round(post))
23                      y = y + 1;
24                  end
25              end
26              xhist(i,t)=x;
27              yhist(i,t)=y;
28              % Dynamics of delay
29              if (input_del(i,t,win)==1)
30                  del = del - b*yhist(i,t);
31              end
32              for z = 1:length(post_spikes_time)
33                  post = post_spikes_time(z);
34                  if (t == round(post))
35                      del = del + a*xhist(i,t);
36                  end
37              end
38              delhist(i,t) = del;
39          end
40          tau(i,win)=round(del);
41          pre_trace_del(win,i)=x;
42          post_trace_del(win,i)=y;
43      end
44
45  end
```